Program for Physiology, Department of Molecular Biosciences
Faculty of Mathematics and Natural sciences
University of Oslo

Effects of hypoxia on angiogenesis and angiogenic factors in crucian carp brain

Master thesis by Miriam Øijordsbakken

Supervisors:

Gøran E. Nilsson

Stian Ellefsen

Christina Sørensen

October 2007

Acknowledgements

I would like to thank my supervisor Gøran Nilsson for having me as a master student in his group, for help, advices and social events during my stay at his laboratory. I am very grateful to Stian Ellefsen and Christina Sørensen for helping me whenever I wrote, called or stopped by their offices. You have been very valuable when I asked all those stupid questions! And thanks to Øyvind Øverli for all the help with statistics.

A special thanks to Helene Kile Larsen and Guro Sandvik, what should I have done without the two of you the first couple of months when Stian was in Liverpool? Also thanks for advices, lunches and parties; it has been a pleasure getting to know you. Thanks to Kristine for encouragement and help, and to Cathrine who had to listen every time something went wrong.

I would like to thank the rest of Gøran`s group for cake meetings, help and social happenings, thanks to everybody at the study room, thanks to Kjell Fugelli for arrangement of seminars, and many thanks to the rest of the people at the Program for Physiology.

My sincere thanks also go to the Department of Oral Sciences Pathology and Forensic Odontology, University of Bergen for all the help with immunohistochemistry.

I am grateful to my two handball coaches during these years, Jørn Mathisen and Jonas Wille for making it possible to combine my biggest sports interest with my education! It means a lot that you have faith in me although I have not been there all the time.

I wish to express my warmest thanks to my family and friends for all help and support, and specially my mum, for her interest in my work for continously giving me unlimited support. I am very fortunate to have a person with your resources in my family!

Oslo, 02.10.2007

Miriam Øijordsbakken

Abstract

Most vertebrates depend on an uninterrupted supply of oxygen to maintain the energy production. Some species, like the crucian carp *(Carassius carassius)* can survive hypoxia for an extended period. This fish is an expert in acquiring the little oxygen that exists in hypoxic water, and can boost its anaerobic ATP production by up-regulating the glycolysis and convert lactate to ethanol.

Angiogenesis, the formation of new blood vessels, is induced by hypoxia and controlled through several factors. One of the most important hypoxia driven transcription factors, the hypoxia-inducible factor (HIF)-α, has been found to play a major role in coordinating many adaptive responses to hypoxia. It is continuously synthesized and degraded in normoxic conditions, but accumulates at low oxygen tension. Several factors control the expression of HIF-α, among them the factor-inhibiting HIF-1 (FIH-1). One mechanism by which HIF-α mediates increased oxygen delivery is through inducing the expression of vascular endothelial growth factor (VEGF), which in turn stimulates the formation of blood vessels.

In this thesis mRNA levels of HIF-1α, HIF-2α, FIH, VEGFA, VEGFC and VEGFD were quantified by real-time RT-PCR in brain tissue from the crucian carp exposed to hypoxia. The effect of hypoxia on vascular density in crucian carp brain was also studied.

A significant increase in mRNA levels was seen in both VEGFA and VEGFC, while no change was seen in VEGFD. VEGFA increased 6-fold and constituted the largest part of the quantified VEGF expression. Different splice isoforms of VEGFA have previously been characterized in mammals and fish, and two of these splice isoforms were cloned in the crucian carp, $VEGFA_{121}$ and $VEGFA_{165}$. A trend towards a reduction in VEGFD expression was observed in hypoxia, which may indicate that it does not have the same function in angiogenesis in crucian carp as VEGFA and VEGFC.

The expression level of FIH increased 4-fold in hypoxia. No changes in mRNA levels were seen in either HIF-1α or HIF-2α, but a trend towards reduction was seen in HIF-1α. The increase seen in VEGFA and FIH indicates that the fishes have been hypoxic. This might imply that the expression of HIF-α also increases, but in order to verify this protein analyses would have to be performed to verify this.

Regarding blood vessel density two parameteres were measured, blood vessel surface area per unit volume and blood vessel length per unit volume. A significant decrease was seen in both of these parameters. The increase in VEGFA expression along with a reduction in blood vessel density can indicate that the hypoxic crucian carp does not require additional blood vessels during hypoxia, but instead suppresses global HIF-α effects, which may work well for local regulation of vascularization, but not for adapting the whole organism to hypoxia.

Table of contents

Abbreviations

ANOVA	analysis of variance
ARNT	aryl hydrocarbon nuclear translocator
ATP	adenosine triphosphate
bHLH	basic helix-loop-helix
Cc	Carassius carassius (crucian carp)
cDNA	complemetary deoxyribo nucleic acid
CBF	cerebral blood flow
CDS	coding domain sequence
C-TAD	COOH-terminal transcriptional activation domain
DAB	3.3′-Diaminobenzidine
EST	expressed sequence tag
FIH	factor inhibiting hypoxia inducible factor
H10	hypoxia exposure 10 days
H10N10	hypoxia exposure 10 days followed by normoxia 10 days
HIF	hypoxia inducible factor
HRE	hypoxia-responsive elements
HRP	horseradish peroxidase
ID	inhibitory domain
IPTG	isopropyl-beta-D-thiogalactopyranoside
mRNA	messenger ribonucleic acid
N10	normoxia exposure 10 days
NF-κB	factor that regulates the expression of the immunglobulin κ light chains in B lymphocytes
NRP-1	neuropilin-1
N-TAD	amino-terminal transactivation domain
OD	optical density
ODDD	oxygen-dependent degradation domain
PAS	Per-ARNT-Sim homology domain
PCR	polymerase chain reaction
PHD2	prolyl hydroxylase domain 2
PPIA	peptidylpropyl isomerase A

RT	reverse transcriptase
SD	standard deviation
S.E.M	standard error of mean
TAD	transactivation domain
VEGF	vascular endothelial growth factor
VEGFR-1	vascular endothelial growth factor receptor 1
X-Gal	5-bromo-4-chloro-3-indolyl-beta-D-galactopyranoside

1 Introduction

Most vertebrates depend on continous oxygen supply for fundamental processes such as energy production. How organisms tolerate conditions of limiting oxygen supply (hypoxia) to cells and tissues vary widely among species (Hochachka and Lutz, 2001). An important factor is where they live. Living in water increases the possibility of encountering hypoxia, primarily because the amount of oxygen contained in a given volume of water is only $1/30^{th}$ of the amount contained in the same volume of air. Further, the rate of diffusion of oxygen in water is 10 000 times slower than in air (Nilsson and Renshaw, 2004). The crucian carp *(Carassius carassius)* often lives in small ponds, and during winter the water becomes anoxic since photosynthesis is blocked due to the ice cover (Nilsson and Renshaw, 2004).

Vertebrates that live in habitats where hypoxia is regularly encountered have evolved physiological and behavioural mechanisms to cope with such challenges. The best studied examples of anoxia-tolerant vertebrates are the crucian carp and some species of North American freshwater turtle, particulary *Trachemys scripta* and *Chrysemys picta* (Nilsson and Lutz, 2004). The turtles have evolved their anoxia tolerance in response to overwintering in anoxic mud at the bottom of lakes. While turtles are comatose during anoxia, the crucian carp stay active (Nilsson, 2001). This allows the crucian carp to move to oxygen rich locations or the water surface to gulp air.

1.1 Physiological adaptations to anoxia in the crucian carp

The crucian carp has several strategies for coping with low oxygen supply. It is an expert in acquiring the little oxygen that exists in hypoxic water. For instance, the haemoglobin of the crucian carp shows an extreme high affinity for oxygen (Sollid et al., 2005).

An impressive quality of the crucian carp is the ability to change the morphology of the gills to increase the respiratory surface area approximately 7.5 times when exposed to hypoxia (Sollid et al., 2003). The respiratory units of the fish, its gill lamellae, becomes protruding after 7 days in hypoxic water due to apoptotic death of cells that cover much of the lamellar surface during normoxia (Sollid et al., 2003).

The capacity for anoxic survival is extended over a wide temperature range. At temperatures close to 0°C the crucian carp can survive anoxia for several months, while at room temperature it can tolerate anoxia for at least a day or two (Nilsson and Lutz, 2004).

Providing sufficient amounts of ATP for cellular processes is a major challenge at low oxygen accessibility. During hypoxia, oxidative phosphorylation stops, and leaves the cell with glycolysis as the only major ATP producing process (Nilsson, 2001).

In crucian carp, the brain blood flow rate more than doubles during anoxia and remains elevated for the entire anoxic period (Nilsson et al., 1994). A similar increase in blood flow also occurs in the anoxic freshwater turtle brain (Hylland et al., 1994), but in this situation the increase is only temporary, and the blood flow starts to fall back to pre-anoxic values within 100 minutes as the turtle enters its comatose state. The increased blood flow is thought to be needed to supply glucose to the brain (Lutz and Nilsson, 1997).

Lactate is the end-product of anaerobic ATP production for all vertebrates. However, genus *Carassius* (Johnston and Bernard, 1983; Shoubridge and Hochachka, 1980). Fishes produce ethanol as the major glycolytic end-product during severe hypoxia and anoxia. By releasing the ethanol to the water through the gills by diffusion, the crucian carp avoids the problem of self-intoxication and end-product build-up, and the high lactate levels and consequent acidosis faced by other vertebrates. The ability to produce ethanol allows *Carassius* to maintain a high glycolytic rate for long periods without having to suffer from enormous lactate loads- an opportunity that is not available to the turtle (Lutz and Nilsson, 1997).

Surviving severe hypoxia/anoxia based on glycolytically produced ATP is energetically very costly, so the crucian carp is dependent on its glycogen stores (Nilsson, 1990). It is known that the crucian carp has the largest store of glycogen of any vertebrate (Lutz and Nilsson, 1997).

It is important to keep in mind that the crucian carp is well-adapted to survive hypoxia or anoxia. This situation is opposite to that in the mammalian brain, where death is the norm in anoxia. Any experimental attempts to extend anoxic survival by boosting or blocking a particular mechanism in a mammal are likely to be hampered by failures of other functions. In mammals, anoxia is synonymous with catastrophe, and a major problem with studying the anoxic mammalian brain is that the physiological changes are very rapid and complex, making it extremely difficult to sort out damaging events from useful defense mechanisms (Nilsson and Lutz, 2004).

1.2 Angiogenesis

Hypoxia induces multiple systemic responses including angiogenesis, erythropoiesis and glycolysis (Haddad, 2002). When hypoxic exposure is prolonged for more than a day or so, the increase in cerebral blood flow (CBF) becomes attenuated (Xu et al., 2004), so that by three weeks of hypoxia exposure the CBF has returned to the prehypoxic baseline. One possible reason for the renormalization of CBF is the observation that the packed red cell volume increases with exposure to hypoxia (Lenfant and Sullivan, 1971). This means that the oxygen content of the circulating blood has been restored by balancing the loss of oxygen with increased carrier, so that the oxygen delivery can be restored at the prehypoxic blood flow rate (Shi et al., 2006). Blood hematocrit has been shown to increase in mammals (Drew et al., 2004). Brain blood flow has also been shown to increase in hypoxic crucian carp (Nilsson et al., 1994).

One of the most important hypoxia driven factors, the hypoxia-inducible factor (HIF)-1α, plays a major role in coordinating many adaptive responses to hypoxia in mammals (Lutz and Nilsson, 2004). In order to respond rapidly to hypoxia, cells continously synthesize, ubiquitinate and degrade HIF-1α under normoxic conditions (Hirota and Semenza, 2006). When the oxygen level drops, this protein escapes degradation and accumulates.

HIF-1α is an important mediator for increasing the efficiency of oxygen delivery through inducing the expression of vascular endothelial growth factor (VEGF), which in turn stimulates the formation of blood vessels. A well-controlled process of adaptations to hypoxia enables oxygen to be delivered more efficiently, through upregulation of VEGF and the expression and activation of other mechanisms such as glucose transporters and glycolytic enzymes (Haddad, 2002).

In mammals almost every cell is located within 50-100 μm of a capillary to ensure adequate oxygen supply (Alberts B. et al., 2002). What mechanism ensures that the system of blood vessels ramifies into every corner? It is endothelial cells that respond to signals produced by the tissue that they invade. A shortage of oxygen in the cells causes an increase in the intracellular concentration of HIF-α, which stimulates transcription of VEGF, and leads to angiogenesis. Angiogenesis is the growth of new blood vessels from pre-existing vessels. In a healthy body it is needed for restoring blood flow to tissues after injury or insult. In females, angiogenesis also occurs during the monthly reproductive cycle and during pregnancy (Ferrara et al., 2003).

Angiogenesis is controlled through several factors. These can be grouped into the "on-switches" including hypoxia-inducible factor 1 and 2 (HIF-1 and -2), and "off-switches" including factor inhibiting HIF (FIH). There is a continous balance between the on-switches and off-switches, and generally angiogenesis is turned off due to the production of more inhibitors than stimulators.

Angiogenesis is essential for several pathological conditions. If the formation of blood vessels is disregulated, this can contribute to numerous malignant, ischemic, inflammatory, infectious and immune disorders (Carmeliet, 2003). Both HIF and VEGF are upregulated in a number of diseases, making them interesting targets for angiogenesis inhibition as a therapeutic strategy (Ho and Kuo, 2007). Therefore, an anti-VEGF strategy is currently being used in various clinical trials to treat tumour patients with the aim of inhibiting tumour-induced angiogenesis, thereby depriving the tumor cells of nutrients and oxygen (Korsisaari et al., 2007). Thus research on angiogenesis and the factors involved has attracted considerable attention recently.

Lymphangiogenesis results in the formation of a vascular network distinct from arteries and veins that serves to drain interstitial fluid from surrounding tissues (Kuchler et al., 2006). It plays a pivotal role in immune responses, since leukocyte traffic via the lymphatic vessels to lymph nodes is essential for antigen presentation, and in cancer biology, since tumor cells can spread via the lymph- and blood vessels to establish distant metastases (Baldwin et al., 2005). In mammals, lymph vessels are lined by endothelial cells possibly sprouting from embryonic veins, and their development appears to be critically dependent on the function of PROX1 (a homeobox gene and a specific marker of a subpopulation of endothelial cells) (Wigle and Oliver, 1999) and on VEGFC signalling (Karkkainen et al., 2004).

1.3 Hypoxia inducible factor (HIF)

HIF is a transcription factor, and is a main regulator of gene expression in response to hypoxia. It consists of an α- and a β-subunit. There are three types of α-subunits, HIF-1α, HIF-2α and HIF-3α (Ratcliffe, 2007), of which HIF-1α is the best characterized. In contrast to HIF-1α and HIF-2α, HIF-3α has more restricted expression patterns. HIF-1α and HIF-2α show a 48% amino acid sequence similarity, they are both hypoxia-induced and they have overlapping expression pattern (Hu et al., 2003). To function as transcription factors, both HIF-1α and HIF-2α need to form a dimer with HIF-β, also known as aryl hydrocarbon nuclear translocator (ARNT). The dimers, named HIF-1α and HIF-2α, bind to DNA and upregulate the expression of a largely shared group of target genes. In addition to the amino-terminal basic helix-loop-helix (bHLH) and Per-ARNT-Sim homology (PAS) domains, the HIF-α`s possess two transactivation domains (TADs), separated by a region termed the inhibitory domain (ID), which is responsible for normoxic repression of TAD activity. Overlapping the amino-terminal TAD (N-TAD) is an oxygen-dependent degradation domain (ODDD), which confers normoxic instability to the HIF-α proteins (Bracken et al., 2003) (figure 1.1).

It was proposed earlier that HIF-1α is ubiquitously expressed, while HIF-2α is detected in vascular endothelial cells where it activates the transcription of VEGF (Elvert et al., 1999). Later it has been shown that HIF-2α is involved in the expression of other genes as well (Gordan et al., 2007; Hu et al., 2003).

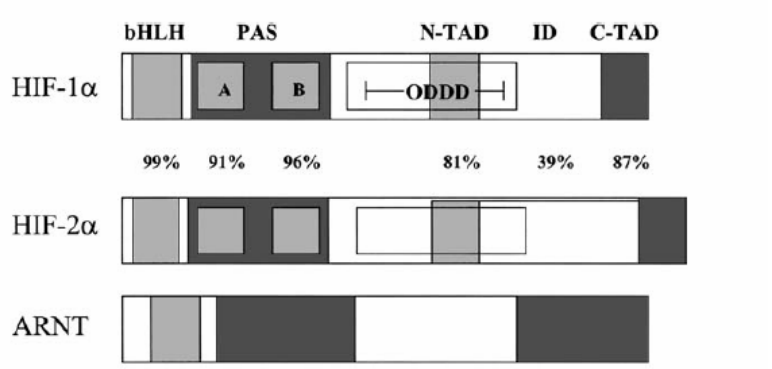

Figure 1.1. *HIF-1α, HIF-2α and ARNT (HIF-1β) domain structure. HIF-1α, HIF-2α and ARNT are basic helix-loop-helix/Per-ARNT-Sim homology (bHLH/PAS) transcription factors. In addition to the carboxy-terminal transactivation domain (C-TAD), similar to ARNT, HIF-1α, HIF-2α also possess an additional amino-terminal transactivation domain (N-TAD), an inhibitory region (ID) that negatively TAD activity and an oxygen-dependent degradation domain (ODDD) that mediates oxygen-regulated stability. From (Bracken et al., 2003).*

In contrast, HIF-3α may function as an inhibitor that is involved in the negative regulation of transcriptional responses to hypoxia (Hirota and Semenza, 2006).

Gene expression mediated by HIF is oxygen sensitive, in part because HIF-α is rapidly degraded in normoxic conditions but stable in hypoxia (Sollid et al., 2006). In normoxia, HIF-α is hydroxylated and recognized by the von-Hippel-Lindau protein, ubiquitinated and then degraded via the proteasomal pathway (Sollid et al., 2006). When the cells become hypoxic, the stabilized HIF-α enters the nucleus and dimerizes with ARNT. The dimers bind to HRE (hypoxia-responsive elements) in the promoter/enhancer region of the target genes, and thereafter interact with transcriptional co-activators.

Activation of HRE leads to upregulation of several genes, including VEGF (Spike et al., 1998). In part, the oxygen sensitivity of HIF function is caused by oxygen-dependent hydroxylation of a spesific asparagine residue near the C-terminus of HIF-α. The asparagine residue is required for interaction with co-activator CBP/p300, which cannot occur if the amino acid is hydroxylated. This hydroxylation event is catalyzed by an asparaginyl hydroxylase, also known as factor-inhibiting HIF-1 (FIH-1) (figure 1.1).

Thus, while the hydroxylation of two proline residues by prolyl hydroxylases (PHD2) earmarks the protein for degradation, FIH possesses an asparaginyl hydroxylase activity that by targeting Asn^{803} (HIF-1α) or Asn^{851} (HIF-2α) (Stolze et al., 2004) represses HIF-α transcriptional activity by preventing binding of the transcriptional coactivator CBP/p300 to the HIF-α C-TAD (COOH-terminal transcriptional activation domain) (Dayan et al., 2006). Silencing of either PHD2 or FIH in normoxia partially induces hypoxic genes, whereas combined PHD2/FIH silencing generate a full hypoxic gene response. FIH does not influence HIF-α stability but allows for modulation of HIF-α transactivation (Dayan et al., 2006).

In crucian carp, HIF-1α levels are affected by both oxygen and temperature. Rissanen et al. (2006a) showed that hypoxia initially increased the HIF-1α protein in all studied tissue at different temperatures except for liver at 18°C, but HIF-1α activity increased only in the heart of 8°C acclimated fish and in the gills of 18°C acclimated fish. They also found that HIF-1α mRNA levels at 8°C increased in the gills and in the kidney, and that it also increased at 26°C in the gills (Sollid et al., 2006).

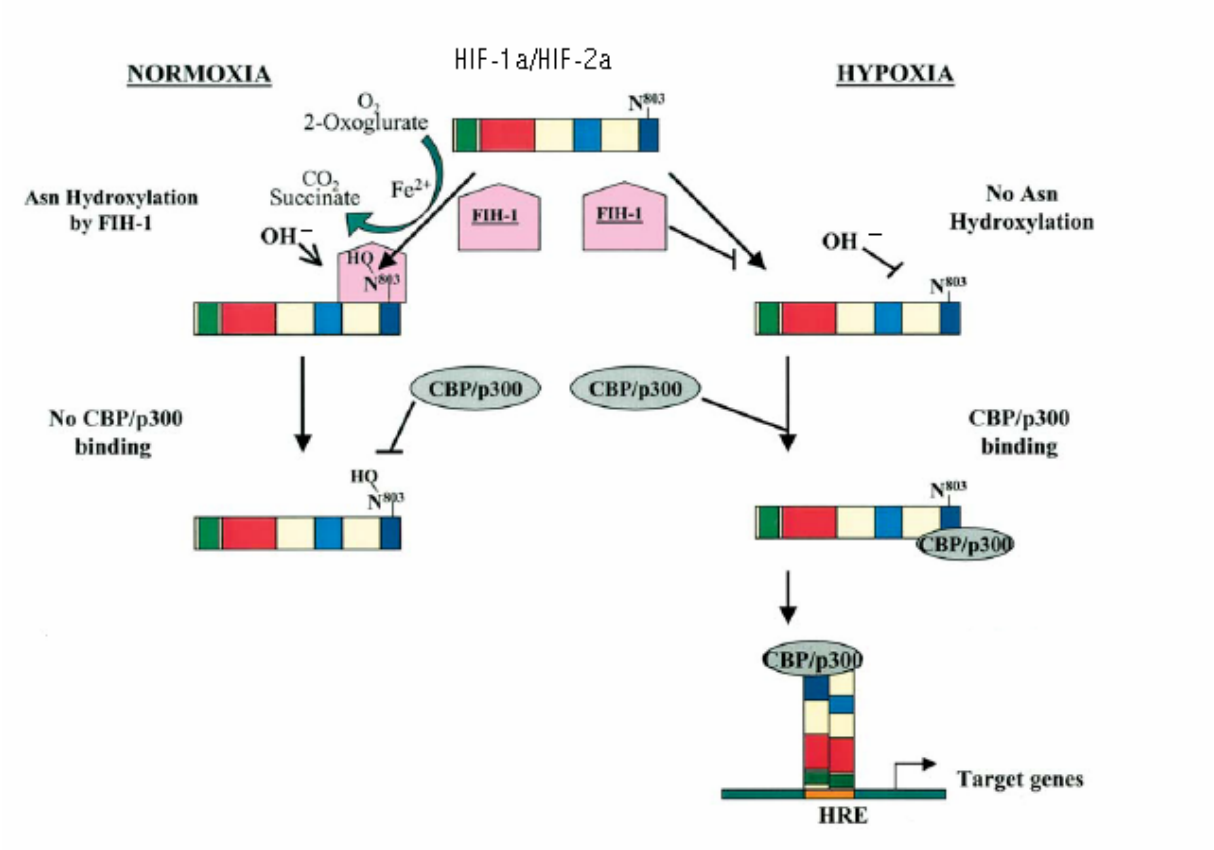

Figure 1.2. *Oxygen -regulated transcriptional activation of HIF-1α and HIF -2α. In normoxia, an oxygen 2-oxoglutarate and iron- dependent HIF-α asparaginyl hydroxylase (FIH-1) binds and hydroxylates specific asparagine residues of HIF-1α (N803) and HIF-2α (N851). This blocks recruitment of transcriptional coactivators (CBP/ p300) by the carbox- terminal transactivation domain (C-TAD), resulting in transcriptionally inactive HIF-α. In hypoxia, FIH-1 activity is blocked due to oxygen deficiency, resulting in no asparagine hydroxylation, and consequently enhanced coactivator recruitment and target gene induction. Modified from (Bracken et al., 2003).*

HIF-2α, but not HIF-1α, interacts with the NF-κB essential modulator (NEMO). NF-κB is a dimeric transcription factor that was first identified as a factor which regulates the expression of the immunoglobulin κ light chains in B lymphocytes. It is also recognized as a sequence-specific transcription factor involved in the activation of a large number of genes in response to inflammation, viral and bacterial infections, and other stressful situations requiring rapid reprogramming of gene expression, such as oxidative challenge (Haddad, 2002).

The interaction between HIF-2α and NEMO enhances normoxic HIF-2α transcriptional activity, independently of the HIF-2α transactivation domain, consistent with a model by which NEMO aids CBP/p300 recruitment to HIF-2α. In contrast, HIF-2α

overexpression does not alter NF-κB signaling, suggesting that the functional consequence of the HIF-2α/NEMO interaction is limited to the HIF pathway. The specificity of NEMO for HIF-2α represents one of the few known differential protein-protein interactions involving HIF proteins, which has important implications for the activity of HIF-2α (Bracken et al., 2003)

Changes in HIF-1α most often occur at the protein level, but can also be seen at the mRNA level (Sollid et al., 2006; Wang et al., 1995). Sollid et al. (2006) have shown that the HIF-1α protein accumulates in the hypoxic crucian carp, and that the mRNA levels followed the protein level trend.

1.4 Vascular endothelial growth factor (VEGF)

VEGF was originally identified as an endothelial cell specific growth factor stimulating angiogenesis and vascular permeability, which is required for the growth and differentiation of endothelial cells (Byrne et al., 2005). More recent studies report that VEGF affects a number of other cell types too (e.g. monocytes, macrophages, neurons, cancer cells, kidney epithelial cells). VEGF was first described by Senger et al. (1983). Further characterization resulted in a publication describing some details of the protein (Senger et al., 1986). However, the protein structure and amino acid sequence of this factor was not described until 1990 (Senger et al., 1990).

The VEGF family plays a key role in angiogenesis. It is important in physiological conditions like endometrial growth, reproductive functions in adults etc. as well as in pathological conditions like diabetic retinopathy and tumor cell growth. It also has an important role in lymphangiogenesis (Roy et al., 2006b).

VEGF has been shown to be of great importance during development, both in vasculogenesis and in angiogenesis. Deletion of either a single or both alleles of VEGF in mice results in embryonic lethality (Ferrara et al., 2003; Li et al., 2007), but overexpression of VEGF also leads to this. These results underline the importance of proper blood vessel formation (Maharaj and D'Amore, 2007). On the other hand, the function in normal adult tissue is poorly understood. In tissues characterized as having a barrier function like the brain (blood-brain barrier), relatively few cells express VEGF (Maharaj and D'Amore, 2007).

HIF directly activates transcription of the VEGF gene (Cai et al., 2003). HIF binds to an HRE in the VEGF promoter region (Hirota and Semenza, 2006), and thereby upregulates VEGF trancription in hypoxia (Storkebaum et al., 2004).

The human VEGF gene is located on chromosome number 6 and is organized in eight exons. (Ferrara et al., 2003). Expression of VEGF is stable in tissue that is angiogenic, but not in tissue like cerebellum, prostate, pancreatic islets and glomeruli (Woolard et al., 2004).

In mammals, the VEGF family comprises seven secreted glycoproteins that are designated VEGFA, VEGFB, VEGFC, VEGFD, VEGFE, VEGFF and the placental growth factor (PIGF). The vascular endothelial growth factors exert their angiogenic role through their receptors which are located on the endothelial cells of blood vessels. These receptors are transmembrane tyrosine kinases which upon binding of their ligands to the extracellular domain of the receptor activate a cascade of downstream proteins (figure 1.3). The receptors involved are VEGF receptor-1 (VEGFR-1), VEGF receptor-2 (VEGFR-2), VEGF receptor-3 (VEGFR-3) and the neurophilins (NRP-1 and NRP-2). The neurophilins lack tyrosine kinase activity and must therefore interact with other receptors to transduce signalling. It also appears that the receptors interact with each other in order to enhance signalling (Otrock et al., 2007b).

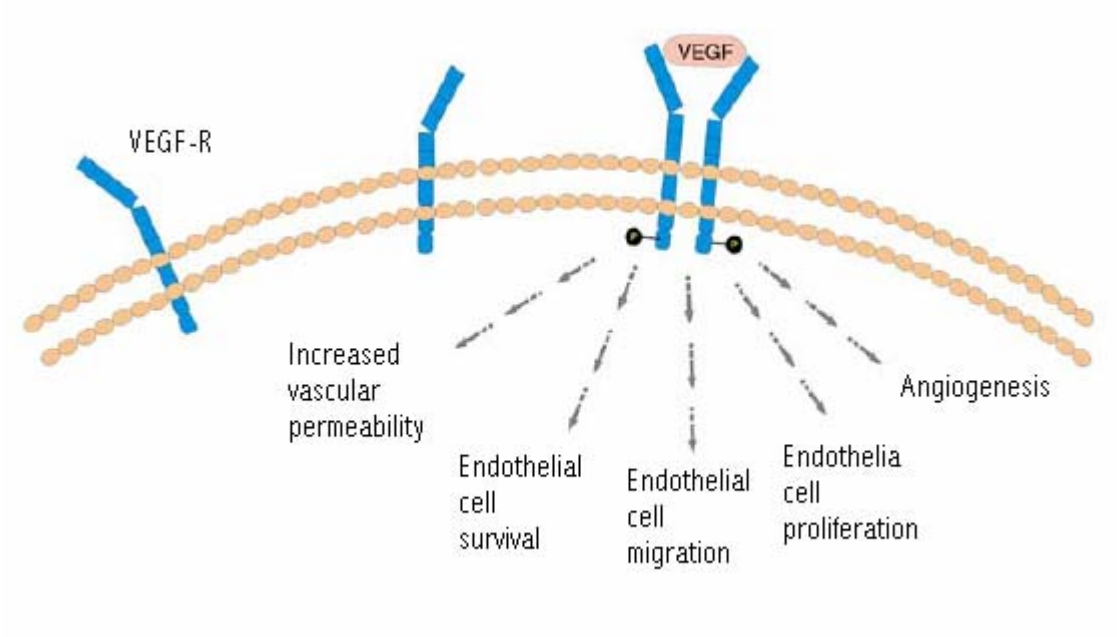

Figure 1.3. *VEGF and its receptor. VEGF binding to its receptor leads to receptor dimerization and activation of receptor tyrosine kinases by autophosphorylation. This leads to several biological effects on endothelial cells. Modified from (Otrock et al., 2007b).*

This thesis focuses on VEGFA, VEGFC and VEGFD, because VEGFA in mammals has been shown to be the most important in the family when it comes to angiogenesis, which is the emphasis of this thesis. VEGFC and VEGFD are involved both in angiogenesis and in lymphangiogenesis (Byrne et al., 2005). These are the reasons why this thesis focuses on VEGFA, VEGFC, and VEGFD.

1.4.1 VEGFA

VEGFA is a key molecule in the induction of angiogenesis and vasculogenesis (the process of blood vessel formation occuring by *de novo* production of endothelial cells), and it is the best characterized and most studied member of the VEGF family (Otrock et al., 2007a).VEGFA mediates its responses primarily by activating VEGFR-1 and VEGFR-2, expressed in vascular endothelial cells, but it also binds to NRP-1 and NRP-2 which are expressed in vascular endothelium and neurons.

In humans alternative exon splicing of the VEGFA gene results in at least 6 different isoforms, the most common being 121, 145, 165, 183, 189 and 206 amino acids long (Roy et al., 2006b). These isoforms have distinct but overlapping functions in VEGFA controlled angiogenesis due to their differential binding to VEGFA receptors. The $VEGFA_{165}$ isoform is the most potent promoter of stimulating angiogenesis. Recently, an alternative variant of $VEGFA_{165}$, $VEGFA_{165}b$ has been identified in mammals. This variant contains an alternative sequence in exon 8, encoding 6 amino acids. In contrary to all other VEGFA isoforms, $VEGFA_{165}b$ is an inhibitor of angiogenesis, counteracting VEGFA-induced proliferation and migration of endothelial cells (Byrne et al., 2005). Although the VEGFA gene structure and regulation are well characterized in human and mouse, no such information is available in fish. Two VEGFA isoforms have been found in zebrafish, $VEGFA_{121}$ and $VEGFA_{165}$ (Bahary et al., 2007). $VEGFA_{165}$ is the dominant isoform in embryos, while $VEGFA_{121}$ is the dominant isoform in adult tissues, indicating possible functional differences between these two isoforms (Gong et al., 2004).

1.4.2 VEGFC

VEGFC induces mitogenesis, migration and survival of endothelial cells. It has long N- and C-terminal extensions as does VEGFD, which the other family members lack. VEGFC

shows similarities to VEGFD concerning receptor specificities (Schena et al., 1998). VEGFC is produced as a precursor protein and is proteolytically activated in the extracellular space by proteases to generate a homodimeric protein with high affinity for both VEGFR-2 and VEGFR-3 (Otrock et al., 2007b). Several studies and knockout models suggest that VEGFC is primarily a lymphangiogenic growth factor, and its lymphangiogenic effects are mediated by VEGFR -3. However, the increase in blood vascular permeability induced by VEGFC is mediated by VEGFR-2 (Roy et al., 2006a).

The existence of a lymphatic system in teleosts (bone fish) has been a matter of debate for decades. It has been difficult to document the development of the lymphatic system due to lack of specific markers. Recently it has been shown in zebrafish (*Danio rerio*) the exsistence of a lymphatic system (Yaniv et al., 2006), and the development of these vessels depend on VEGFC and VEGFR-3 signalling (Kuchler et al., 2006).

The promoter of the VEGFC gene has been found to contain putative NF-κB binding sites which suggests that NF-κB may be involved in inducing VEGFC transcription

1.4.3 VEGFD

VEGFD is present in most adult tissues, and it stimulates growth of vascular and lymphatic endothelial cells by signalling through the tyrosine kinase receptors. The mature form has been shown to bind and activate VEGFR-2 and VEGFR-3 in humans, while the mouse VEGFD only binds to VEGFR-3 (Roy et al., 2006b). Nonetheless, VEGFD may induce lymphatic vessel growth in adult life in response to pathological conditions (Otrock et al., 2007b).

VEGFD is structurally 48% identical to VEGFC by virtue of the unique presence of N- and C-terminal extensions as mentioned earlier (Roy et al., 2006b). Recently it was shown that hypoxia-driven vascular development requires the activity of VEGFD (Otrock et al., 2007a).

Recently VEGFD has been cloned in zebrafish (Song et al., 2007). The VEGFD precursor protein contains long N-terminal propeptides and almost complete VEGF homology domain (VHD) region, while it lacks about 80 amino acid residues in the C-terminal. This is different from human and mouse VEGFD (Song et al., 2007).

1.5 Aims of this study

The aims of this study was to examine the effect of hypoxia on the expression of the hypoxia regulated transcription factors HIF-1α, HIF-2α and FIH, and the angiogenesis stimulating factors of the VEGF family in the crucian carp. In addition, the effect of hypoxia on vascular density in crucian carp brain was also studied.

2 MATERIALS AND METHODS

This thesis reports two different experiments; (1) quantification of the expression of genes involved in angiogenesis in normoxic and hypoxic crucian carp brain, and (2) quantification of vascularisation in normoxic and hypoxic crucian carp brain.

2.1 Animal handling

Crucian carps were captured in Tjernsrud pond in Bærum, Norway, in August 2006. Fishes were kept in 750-litre tanks in the aquarium facility of the Department of Molecular Biosciences, University of Oslo. These tanks were continously supplied with aerated and dechlorinated tap water from Maridalsvannet, Oslo. A light/dark-cycle of 12h light/12h darkness was held, and the fish were fed daily with commercial fish food (Tetrapond, Tetra). They were not fed during experiments. Experimental animals weighed 33.2 ± 12 g (first experiment) and 29.0 ± 17 g (second experiment). Male/female fishes were randomly selected.

Two experiments were performed, one in October 2006 for studying gene expression, and one in February 2007 to study vascularisation.

2.2 Hypoxia exposure and tissue sampling

Hypoxia exposures were performed at 9°C, with three exposure regimes; 10 days normoxia (N10), 10 days hypoxia (H10), and 10 days hypoxia followed by 10 days normoxia (H10N10). The experiments were performed in 25-litre circular tanks, with 23 fish in each tank. These tanks were supplied with dechlorinated tap water. De-oxygenation was obtained by N_2-bubbling, and oxygen levels were monitored using two galvanometric oxygen electrodes connected to a computer (figure 2.1).

Prior to the exposure, fishes were left to acclimate in the 25-litre tanks for 24 hours, followed by removal of excrements and closure of tanks with tight lids.

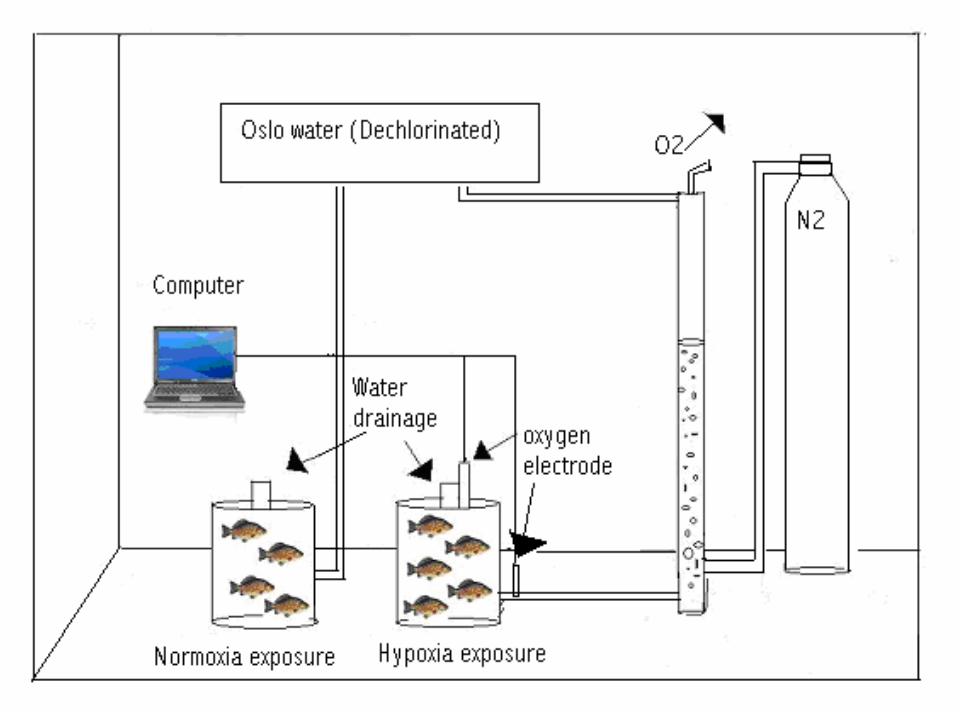

Figure 2.1. *Experimental set-up. Left circular tank represents normoxia experiment, while right tank represents hypoxia experiment. The oxygen level and temperature were registered by oxygen electrodes, and recorded by a computer.*

Fishes were killed by stunning them with a sharp blow to the head, before cutting the spinal cord and dorsal aorta, and removing the brain. Within 30 s of capture, brains were removed, and snap-frozen in liquid N_2. The brains were stored at -80ºC.

For the immunohistochemical experiment, the brains were cut in half between optic tectum and cerebellum and fixed in 4% phosphate buffered formalin (pH 7) (table 2.1)

Table 2.1. *Number of fish in each exposure group*

Time of exposure	**Temp (°C)**	**state of oxygenation and days of exposure (=n)**			**organ**	**Purpose**
October 2006	9	N10 (6)	H10 6)	H10N10 (6)	brain	gene expression
February 2007	9	N10 (5)	H10 (9)	H10N10 (6)	brain	histology

2.3 Isolation of total RNA with TRIzol® Reagent

The dissected brains were weighed in frozen condition (108.1 ± 23.1 mg) and quickly transferred to a tube placed on ice, containing 500 µl TRIzol (Invitrogen, Carlsbad, CA, USA). Total RNA from brain tissue was isolated according to the manufacturer`s protocol (Invitrogen, Carlsbad, CA, USA). An electrical homogenizer (Ultra-Turrax T8, IKA) was used to homogenize the brain tissue.

2.4 Quality check of total RNA

The quality of all total RNA samples were verified by analyzing 1 µl of 1:10 dilutions on a 2100 Bioanalyzer in accordance with manufacturer`s protocol (Agilent Technologies, Palo Alto, CA, USA). RNA concentrations were measured using a NanoDrop spectrophotometer (NanoDrop Technologies, Rockland, DE, USA). This was done using 1:10 dilutions of total RNA. Duplicate measurements were performed, and the concentrations were found to be between 540-2500 ng/µl of undiluted total RNA solution. 28S/18S ratios were obtained, but as these are not reliable for quality control of RNA, all inspections of RNA integrity were performed visually (as recommended by Agilent Technologies). This was done by inspection of small and large peaks (such as rRNA and 28S RNA), and comparing peak shapes and assessing baseline flatness. No RNA samples were excluded at this stage.

2.5 DNase treatment and cDNA synthesis

1 µg of total RNA was treated with DNase I (DNA-free^{TM} Kit, Ambion Applied Biosystems, Foster City, CA, USA) prior to cDNA synthesis to avoid any possible contamination of genomic DNA. The DNase enzyme was inactivated, and the supernatant transferred to new tubes.

Reverse transcription was performed using Superscript ^{TM} III Reverse Transcriptase (Invitrogen, Carlsbad, CA, USA) and 500 ng oligo$(dT)_{18}$. Both DNase I and cDNA synthesis were performed according to the manufacturer`s protocol. Two cDNA syntheses were carried out for each RNA sample. The cDNA was diluted 1:25 with DEPC (diethylpyrocarbonate)-milliQ water. All procedures were performed according to manufacturer`s protocol.

2.6 Partial cloning and sequencing of the genes

The genes of interest had not been sequenced in crucian carp prior to this study. It was therefore necessary to partially clone and sequence these to be able to design species specific primers for the real time RT-PCR assay. The following genes were cloned; VEGFA, VEGFC and VEGFD.

Cloning was performed from cDNA of normoxic crucian carp brain tissue. The primers were designed in conserved regions of the genes. These regions were located using alignments of multiple organisms, mouse *(Mus musculus)*, chicken *(Gallus gallus)*, frog *(Xenopus laevis)*, and pufferfish *(Tetraodon nigroviridis/Takafugu rubripes)*, with emphasis on zebrafish (*Danio rerio*). The sequences were available on NCBI`s nucleotide database (http://www.ncbi.nlm.nih.gov/), and alignments were done using Clustal X (version 1.83) and Genedoc (version 2.6.002). Primers were designed using the web-based Primer3 software, (http://frodo.wi.mit.edu/cgi-bin/primer3/primer3_www.cgi) and were synthezised by Invitrogen (Invitrogen, Carlsbad, CA, USA). All primers had a melting temperature around 60°C. See table 2.2 for primer sequences.

PCR was performed on 1:25 dilutions of the resulting cDNA using Platinum Taq polymerase (Invitrogen, Carlsbad, CA, USA). The following PCR program was used: 94°C for 10 min, 94°C for 30 sec, 50°C for 1 min, 72°C for 1 min, repeats steps 2-4 45×, 72°C for 10 min, hold 4°C.

PCR-reactions were analyzed by electrophoresis on 1 % agarose-gel containing EtBr (BHD-electron). Resulting dsDNA fragments were ligated into pGEM® -T easy Vector System I (Promega, Madison, WI, USA). Ligation reactions were transformed into $CACl_2$-compentent cells (TOP10 F; Invitrogen, Carlsbad, CA, USA), and afterwards applied on IPTG/X-gal agar plates. Colony PCR were performed on 6-8 colonies, using M13 forward and M13 reverse primers (Invitrogen, Carlsbad, CA, USA). Selection was based on the colour of the colonies. White colonies were picked because they had the desired insert, while blue colonies did not have this. Sequencing of the colony PCR-product was done using T7 primers at the ABI-lab at CEES, Department of Biology and Molecular Biosciences, University of Oslo, according to manufacturer`s protocol.

All sequences are listed in appendix III.

Table 2.2. *Primers used in initial gene fragment cloning*

Gene	Forward primer 5` → 3`	Reverse primer 5` → 3`
VEGFA F1R1	GGCTCTCCTCCATCTGTCTG	TGCATTCACACTTGGTGTGTT
VEGFC F2R2	TTGGGGCTACAAACACCTTC	TCTCTTGGGGTCCACGTTAC
VEGFD F2R2	TGGACTTCACATGTTGCTTCTC	TCGCTCTACATCCATCTCACA

2.7 Obtaining the 3′ end of VEGFA

Variable splice cassettes of VEGFA are located at the 3′ end of this gene. The isoform $VEGFA_{165}$ is of special interest, because an inhibitory variant, $VEGFA_{165}b$ has been identified in mammals (Woolard et al., 2004). Two different approaches were performed to obtain sequences from the VEGFA 3′ end. The two methods used were RACE and PCR to obtain expressed sequence tag (EST).

2.7.1 Obtaining complete cDNA sequences by RACE

RACE was performed on RACE cDNA from crucian carp brain (Cand. Scient. thesis by Dag Are Hov) using GeneRacer^{TM} kit (Invitrogen, Carlsbad, CA, USA). GSPs were designed based on the previously described crucian carp EST (see section 2.6) using the Primer3 software. All GSP RACE primers are listed in table 2.3.

Table 2.3. *Primers used in RACE*

GENE	Forward primer 5` → 3`	Reverse primer 5` → 3`
VEGFA RACE F1R1	TGTCCCTACAGAGACCCGCAACG	GCTGTCAACGATACGCTACGTAACG
VEGFA RACE F2R2	TGTGCAGGCTGCTGCAACGAC	GCTGTCAACGATACGCTACGTAACG
VEGFA RACE F3/ GeneracerTM 3′nested primer	ACAGAGACCCGCAACGTCACC	CGCTACGTAACGGCATGACAGTG
VEGFA RACE F3/ nested primer 3	ACAGAGACCCGCAACGTCACC	CGCTACGTAACGGCATGACAGTG
VEGFA RACE nested primer 1/nested primer 3	TGTGCAGGCTGCTGCAACGAC	CGCTACGTAACGGCATGACAGTG
VEGFA RACE nested primer 2/nested primer 3	ACAGAGACCCGCAACGTCACC	CGCTACGTAACGGCATGACAGTG

The size of the 3′ RACE product was estimated to be 100-400 bp based on known zebra fish sequences. This information was used to set the length of the elongation step. The following PCR program was used: 94°C for 2 min, 94°C for 30 sec, 72°C for 1 min, repeat steps 2-3 5×, 94°C for 30 sec, 70°C for 1 min, repeat steps 4-5 5×, 94°C for 30 sec, 68°C for 30 sec, 72°C for 1min, repeat steps 6-8 35×, 72°C for 10 min, hold 4°C. Nested RACE was performed using the following PCR program; 94°C for 2 min, 94°C for 30 sec, 72°C for 1 min, repeat steps 2-3 5×, 94°C for 30 sec, 70°C for 1 min, repeat steps 4-5 5×, 94°C for 30 sec, 68°C for 30 sec, 72°C for 1min, repeat steps 6-8 35×, 72°C for 10 min, hold 4°C. Cloning and sequencing of all RACE products were performed as described in section 2.6. RACE were performed according to manufacturer`s protocol.

2.7.2 Obtaining $VEGFA_{165}$ by PCR

The crucian carp $VEGFA_{165}$ splice variant was also targeted by using PCR. This implied cloning of an EST from the 3′ end using primers based on the previously described crucian carp VEGFA EST (section 2.6), and reverse primers from zebrafish. Primers are listed in table 2.4.

Table 2.4. *Primers used in $VEGFA_{165}$ cloning*

Gene	**Forward primer 5` → 3`**	**Reverse primer 5` → 3`**
$VEGFA_{165}$ F1R1	ACTGCGAGTCAAACAACGTG	GCTTTGACTTCTGCCTTTGG
$VEGFA_{165}$ F3R1	AAGGGATGAAGGGCAAAAAT	GCTTTGACTTCTGCCTTTGG
$VEGFA_{165}$ F3R3	AAGGGATGAAGGGCAAAAAT	TCTTGGCTTTTCACATCTGC

PCR, cloning and sequencing were performed as described in section 2.6. The following PCR program was used; 94°C for 2 min, 94°C for 30 sec, 72°C for 1 min, 72°C for 2 min repeat steps 2-4 4×, 94°C for 30 sec, 68°C for 1 min, 72°C for 2 min repeat steps 5-7 4×, 94°C for 30 sec, 65°C for 1 min, 72°C for 2 min, repeat steps 8-10 29×, 72°C for 10 min, hold 4°C.

2.8 Quantification of mRNA expression with real-time RT-PCR

Designing primers for real time RT-PCR

β-actin was chosen as internal RNA reference gene based on previous testing of the expression levels in the crucian carp brain under oxidative stress (Ellefsen S. et al., *In prep.*). Gene specific real-time RT-PCR primers were designed from crucian carp sequences using the LightCycler Probe Design Software (version 1.0, Roche). Primers were made for VEGFA, VEGFC and VEGFD, and synthesized by Invitrogen (Invitrogen, Carlsbad, CA, USA).

Three primer pairs were designed for each of the genes of interest. These were tested in a real-time RT-PCR assay with cDNA. The specificity of the primers was verified by cloning and secuencing of the real-time RT-PCR products. See table 2.5 for real-time RT-PCR primers.

Table 2.5. *Primers used for real-time RT-PCR*

Gene	**Forward primer 5` → 3`**	**Reverse primer 5` → 3`**
β-actin	TGTTTGAGACCTTCAACAC	CGGACAATTTCTCTTTCG
VEGFA	ACACCTACATCCCGTC	GTGAAACTCAGTTGAAAATTATGC
VEGFC	TGTAACAGTGAGGAGCAAG	ACACAAGCGATTACTCCAG
VEGFD	GCTGCTGCAACAAAGA	CCAGTCCCATATTAAACCTC
HIF-1α	AATACTATCATGCCCTGG	TGAGAACGTAGTTGACAC
HIF-2α	GTGGATTCAAAGAGCCT	ATAGAACTCATACGCCGA
FIH	GTAAGGATAGAGGCAGTC	TGATACAGTTGGCCGAA

RNA extraction and cDNA synthesis for real-time RT-PCR

Total RNA for real-time RT-PCR experiments was extracted from 65 mg brain tissue (9°C) of crucian carp (Table 2.1) using TRIzol® reagent. The amount of tissue being extracted was determined by the smallest available tissue sample in each experiment. This was achieved by using equal amounts of specific volumes of homogenized TRIzol/tissue mixtures (Ellefsen S. et al., *In prep.*). The aim was to maximize the amounts of extracted RNA and to standardize the procedure. Samples within one series of RNA extraction were handled in a particular order. The handling of each exposure group (N10, H10 and H10N10) shifted continuously. Within each exposure group individual fish were handled at random. The quality and quantity of the total RNA were assessed as described in section 2.4.

Real-time RT-PCR

Quantification of mRNA levels of the genes of interest (see table 2.4) was performed on a Lightcycler® 2.0 instrument, using the LightCycler FastStart DNA Master^{PLUS} SYBR green I kit (Roche Diagnostics, Basel, Switzerland). Two real-time RT-PCR reactions were performed on each gene for each cDNA synthesis to quantify the expression of each gene. Since two cDNA syntheses were carried out for each RNA sample, a total of four real-time RT-PCR reactions were carried out on each gene for each cDNA synthesis.

One adjustment was made; each reaction was halved as described in (Nolan et al., 2006). The following real-time RT-PCR program was used; 94°C for 10 min, 94°C for 10 sec, 60°C for 12 sec, 72°C for 8 sec, repeats steps 2-4 39×. A melting curve analysis was generated according to the manufacturer`s protocol. A melting curve is used to indicate that the PCR reactions contain only one type of PCR product. Melting curves are a powerful mean of providing accurate identification of amplified products and excluding them from primer dimers and other small artefacts (Nolan et al., 2006).

LightCycler PCR for target and reference genes was always run in the same carousel to avoid inter-assay variations. Real-time RT-PCR was performed according to the manufacturer′ s protocol (Roche Diagnostics, Basel, Switzerland).

Data from the LightCycler PCR was visualized in the LightCycler3 Data Analysis program (Roche Diagnostics, Basel, Switzerland). Relative gene expression data were obtained from real-time RT-PCR raw-data using this equation:

$$\frac{\beta\text{-actin}\,E^{Cp}}{\text{Target gene}\,E^{Cp}} \times 100 = \text{expression of target gene in \% of } \beta\text{-actin}$$

where Tar = target gene, Con = control gene, E = priming efficiency and Cp = crossing point (Ellefsen S. et al., *In prep.*).

The crossing point (Cp) was calculated by using the second derivative maximum method (LightCycler Software version 3.5, Roche diagnostics). Cp is a reference point in the PCR reaction curve to correlate the reaction curves to amount of initial starting template. The efficiency (E) was estimated for each PCR reaction using LinRegPCR (version 7.5) (Ramakers et al., 2003). E_{means} was calculated for each real-time RT-PCR primer pair, and were used in calculations of relative gene expression.

2.9 Statistical analyses

The data obtained were tested for normality by the method of Kolmogorov and Smirnov. To test for significant changes in gene expression compared to the control (N10), the two way ANOVA was used. When the data showed significant variation in SD, two ways ANOVA with Tukey post Hoc test was used. $P \leq 0.05$ was considered significant. The statistical calculations were done using GraphPad InStat (GraphPad InStat 3.06, GraphPad Software Inc).

2.10 Immunohistochemical visualisation and quantification of blood vessels

After 48 h of fixation, the tissue was placed in a Tissue-Tek VIP Vacum Infiltrating Processor (Sakura Finetek, USA) for dehydration and paraffin infiltration.

2.11 Sectioning

5 µm transverse sections from the telencephalon (Figure 2.2) were made on a Leica serial cutting machine. Sections were mounted on Menzel gläser SuperFrost (R) Plus (Menzel GmbH & Co KG, Saarbrückener Str. 248, Germany). Sections were placed in an incubator at approximately 58°C for 24 h. The purpose was to make the tissue stick to the glasses to avoid destroying epitopes: the temperature should not be higher than the melting point of the paraffin. Sections were then kept in a refrigerator in a closed box, and used within three months.

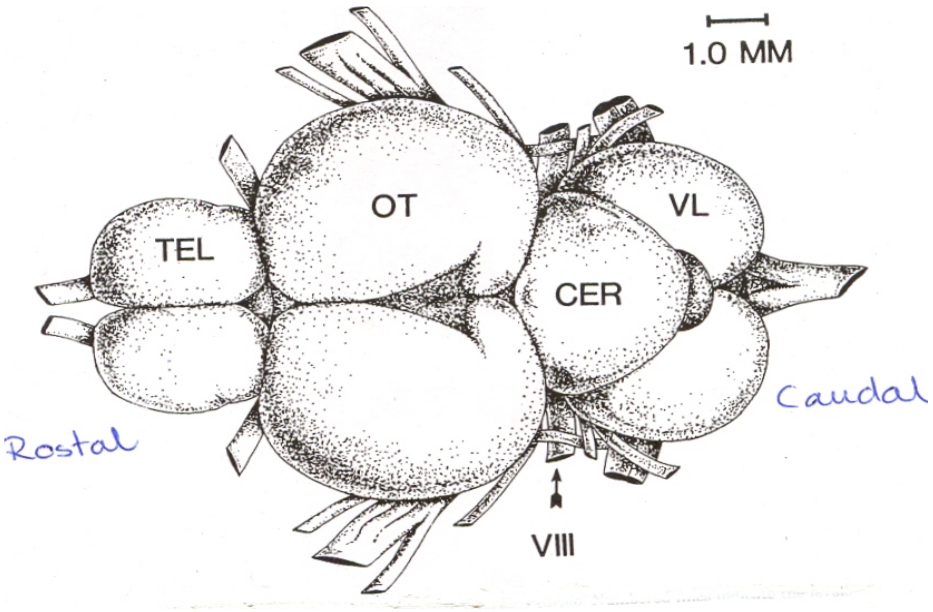

Figure 2.2*. Schematic drawing of the common carp, Cyprinus carpio brain.(TEL; telencephalon, OT; optic tectum, CER; cerebellum, VL; vagal lobe (Echteler, 1984).*

2.12 Laminin

The basement membrane is a structure that supports overlying endothelial cells. It forms a continous sleeve around the endothelial tube in adult tissue, and the interaction of endothelial cells with basement membrane components plays an important role in the maintenance of vessel wall intergrity. The basement membrane of endothelium is composed of laminins (Hallmann et al., 2005). The members of the laminin family of glycoproteins are major constituents of basement membranes (basal lamina) and they are extracellular matrices in dense contact with individual cells and cell layers (Colognato and Yurchenco, 2000).

2.12.1 Staining

To select the appropriate method for detecting the vessels in the brain of the fish, different trial stainings were done; Hematoxylin/Eosin, PAS, Elastin van Gieson and Masson Trichrome. The vessels were stained, but for an untrained person it was difficult to count and measure them. Then different specific antibodies were tested, such as CD31, CD34 and Factor VIII with no result. The reason could be that these markers are for human tissue and not for fish. Anti-Laminin, one produced against human and different animals and one just against human were tested . Both of them gave the same good results, and Polyclonal Rabbit Anti-Laminin from Dako was preferred due to its low price.

Sections were deparaffinized in xylene, rehydrated through graded alcohol to distilled water. For target retrieval Dako Proteinase K (S2019, 40x) was used at room temperature for 5 minutes. Endogenous peroxidase activity was blocked with 0.03 % Dako hydrogen peroxidase (Dako, S2001) for 5 minutes. Sections were incubated with primary antibody (Ab); Polyclonal Rabbit Anti-Laminin 1:400 (Dako, Z0097) for 1 hour in a humidity chamber. The antibody was diluted in Dako Antibody Diluent (Dako, S0809). The primary antibody was followed by a spine molecule (EnVision+ System, Dako, K4011) which contains molecules of secondary antibodies (anti-rabbit) and molecules of horesradish peroxidase (HRP) for 30 minutes. After each step sections were washed twice (2x5 minutes) in Tris-buffered saline (TBS) pH 7.6. Development with 3.3´diaminobenzidine (DAB+, Dako, K3468) in buffered substrate solution containing hydrogene peroxide (H_2O_2) was performed for 12 minutes. Sections were counterstained with hematoxylin (Dako, S3301) for 3 minutes (Figure 2.3). After dehydration xylene sections were mounted with Eukitt (O. Kindler GmbH & Co, Germany).

As negative controls, staining with isotype and concentration matched controls were performed to ensure specific staining (rat Immunoglobulin fractions, DAKO, Denmark). Tonsillar tissue was used as positive control as recommended from Dako.

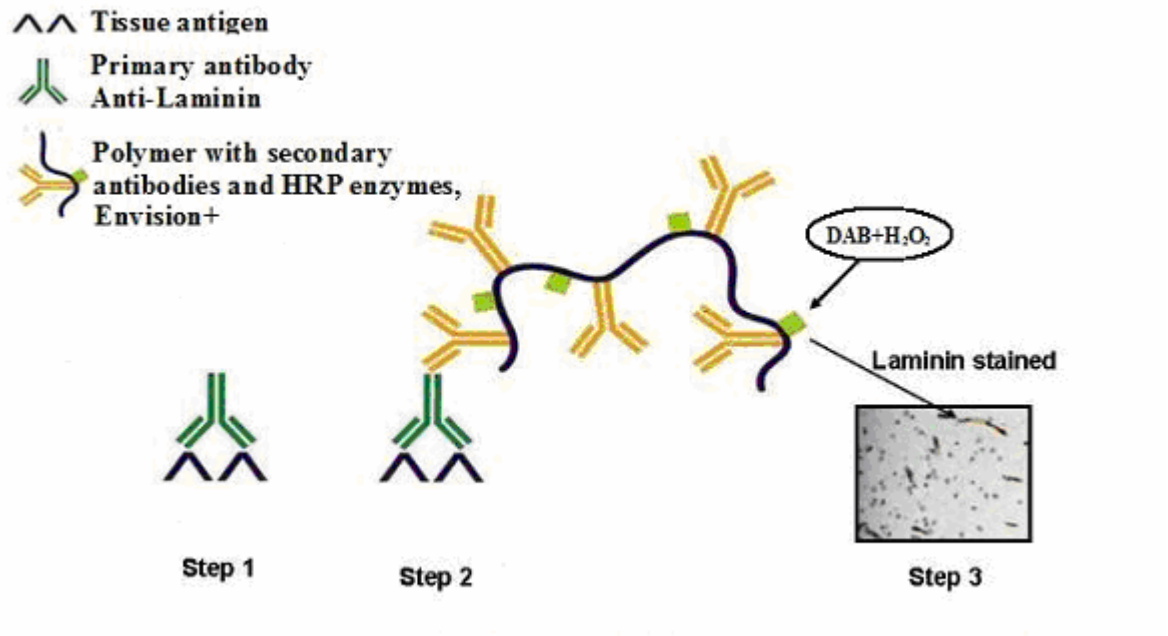

Figure 2.3. *For staining of one tissue marker by EnVision+ System. Primary antibody (step 1), anti-Laminin, is followed by a spine molecule which contains an average of 20 molecules of secondary specific antibodies and 100 molecules of Horseradish Peroxidase (HRP) enzymes (step 2). It is concluded with the use of substrate-chromogen Diaminobenzine (DAB) + H_2O_2 reacting with the HRP enzymes on the spine molecule and staining the positive laminin vessels (step 3). The drawing is modified from Dako Handbook in Immunochemical staining methods, 3rd edition.*

2.12.2 Stereology

Five or six random sections taken from the telencephalon rostrally to the anterior comissure from each animal were investigated using a Zeiss Axioplan 2 imaging microscope. For one animal only 3 sections were investigated due to loss of sections. 2-4 no- overlapping photographs of resolution 2600 x 2060 pixles, corresponding to 680 x 539 µm, were taken from each section. Thus, a total area of 4398240-13194720 μm^2 was analysed from each animal.

The images were analysed using ImageJ software (ImageJ 1.37v, (http://rsb.info.nih.gov/ij/), Wayne Rasband, National Institutes of health, USA). Two parameteres were measured according to methods described by Elias and Hyde (1980); blood vessel surface area per unit volume and blood vessel length per unit volume.

Surface area was measured by superimposing test lines of known length randomly on the images, whereupon the number of times the lines were crossed by the surface of a stained profile was calculated. The resulting value, profiles per unit length of test line, (P_L) was put into formula (1), taken from Elias and Hyde (1980), to obtain surface area per unit volume (S_V).

$$S_V = 2P_L \quad (1)$$

Vessel length was measured by superimposing test squares of known area randomly on the images and counting the number of stained vessels that were contained completely within the square or crossing the top or left sides of the squares. Vessels that crossed the right or bottom sides were excluded. The resulting value, number of profiles per investigated area (P_A) was put into in formula (2), taken from Elias and Hyde (1980), to obtain vessel length per unit volume (L_V).

$$L_V = 2P_A \quad (2)$$

2.13 Statistical analyses

Fish weight and histological data were analysed by two-way ANOVA with sex and treatment (normoxia, hypoxia, hypoxia-normoxia) as independent variables, followed by Tukey-Kramer post-hoc test for unequal n. Correlations between dependent variables (weight, S_v, L_v) were analysed by linear regression. The difference between regression slopes were compared using the t statistics according to the method suggested by Armitage (1980) There was no significant deviation from normality (Komogorov-Smirnov test) or lack of homogeneity of variance (Levene's test) for any dependent variable. Chi-square test confirmed that the frequency of males and females in each experimental group did not differ significantly between groups.

3 Results

The exposure groups are here abbreviated as N10 (normoxia 10 days), H10 (hypoxia 10 days) and H10N10 (hypoxia 10 days followed by normoxia for 10 days).

3.1 Cloning and sequencing of VEGFA, VEGFC and VEGFD

The phylogenetic tree shown in figure 3.1 presents the obtained crucian carp (cc) sequences for VEGFA, VEGFC and VEGFD groups together with previously described sequences from zebrafish (dr).

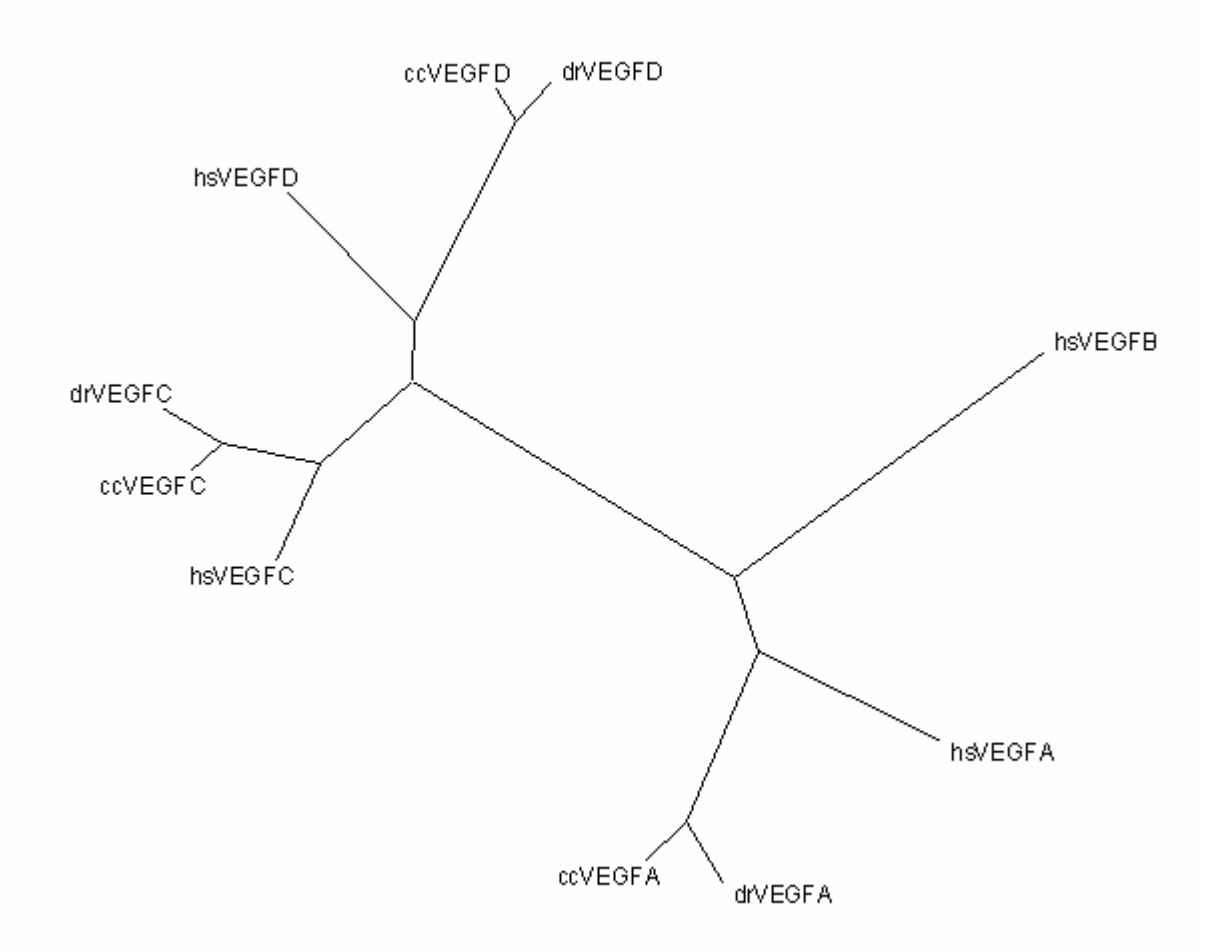

Figure 3.1. *Phylogenetic tree of VEGFA, VEGFB, VEGFC and VEGFD showing the relationsship between the genes in different species. Species included are cc = carassius carassius, dr = danio rerio, hs = homo sapiens*

3.2 Relative mRNA levels of HIF-1α and HIF-2α

Quantification of mRNA levels of the HIF genes were performed on total RNA from crucian carp brains exposed to different oxygen regimes at 9°C. Expression data of each gene was normalized using β-actin as the internal reference gene.

No significant changes in expression were detected in either HIF-1α (Two way ANOVA, P = 0.06) or in HIF-2α (Two way ANOVA, P =0.70) in H10 compared to the N10 group. There were no effects of sex (HIF-1α, P = 0.67, HIF-2α, P = 0.26) (figure 3.2).

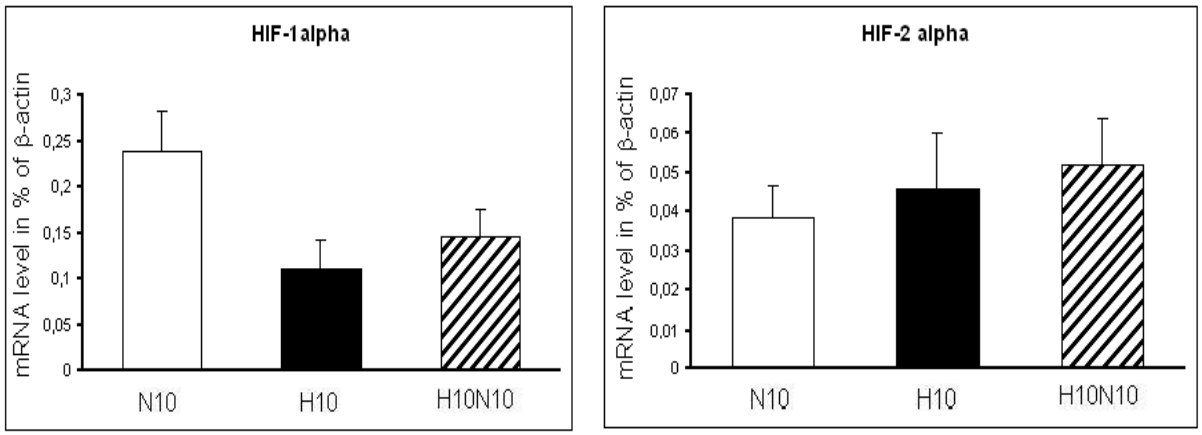

Figure 3.2. *Relative mRNA levels of HIF-1α and HIF-2α in the crucian carp brain, exposed to different oxygen regimes at 9℃. The data is normalized using β-actin as the internal reference gene. For number of fish in each exposure group, see table 2.1. For statistical details, se appendix II.*

3.3 Relative mRNA levels of FIH-1

Quantification of mRNA levels of the FIH-1 gene was performed on total RNA from crucian carp brains exposed to different oxygen regimes at 9°C. Expression data of each gene was normalized using β-actin as the internal reference gene.

FIH-1 showed a significant increase in expression in H10 compared to the N10 group (Two way ANOVA, P = 0.002). Different letters denote significant differences (Tukey post hoc test) (figure 3.3). There was no effect of sex (Two way ANOVA, P = 0.31).

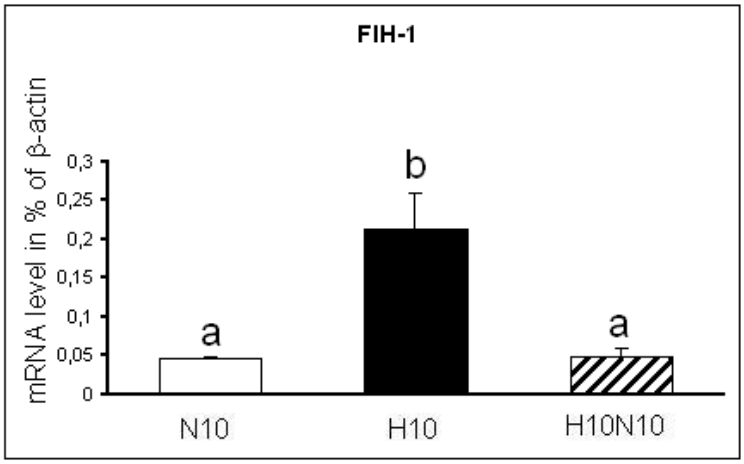

Figure 3.3. *Relative mRNA levels of FIH-1 in the crucian carp brain, exposed to different oxygen regimes at 9℃. The data is normalized using β-actin as the internal reference gene. Different letters denote significant differences (Tukey post hoc test). For number of fish in each exposure group, see table 2.1. For statistical details, se appendix II..*

3.4 Relative mRNA levels of the VEGF genes

Quantification of mRNA levels of the VEGF genes were performed on total RNA from crucian carp brains exposed to different oxygen regimes at 9°C. Expression data of each gene was normalized using β-actin as the internal reference gene.

With regard to the VEGF genes, both VEGFA (Two way ANOVA, P< 0.01) and VEGFC (Two ways ANOVA, P = 0.005) showed a significant increase in H10 compared to N10. Different letters denote significant differences (Tukey post hoc test). There was no significant effect of sex (Two way ANOVA, VEGFA, P = 0.89, VEGFC, P = 0.13) (figure 3.4) in either VEGFA or VEGFC. No significant changes were detected in the expression of VEGFD compared to the N10 group, and no effect of sex in VEGFD was seen (Two way ANOVA, P = 0.94) (figure 3.4).

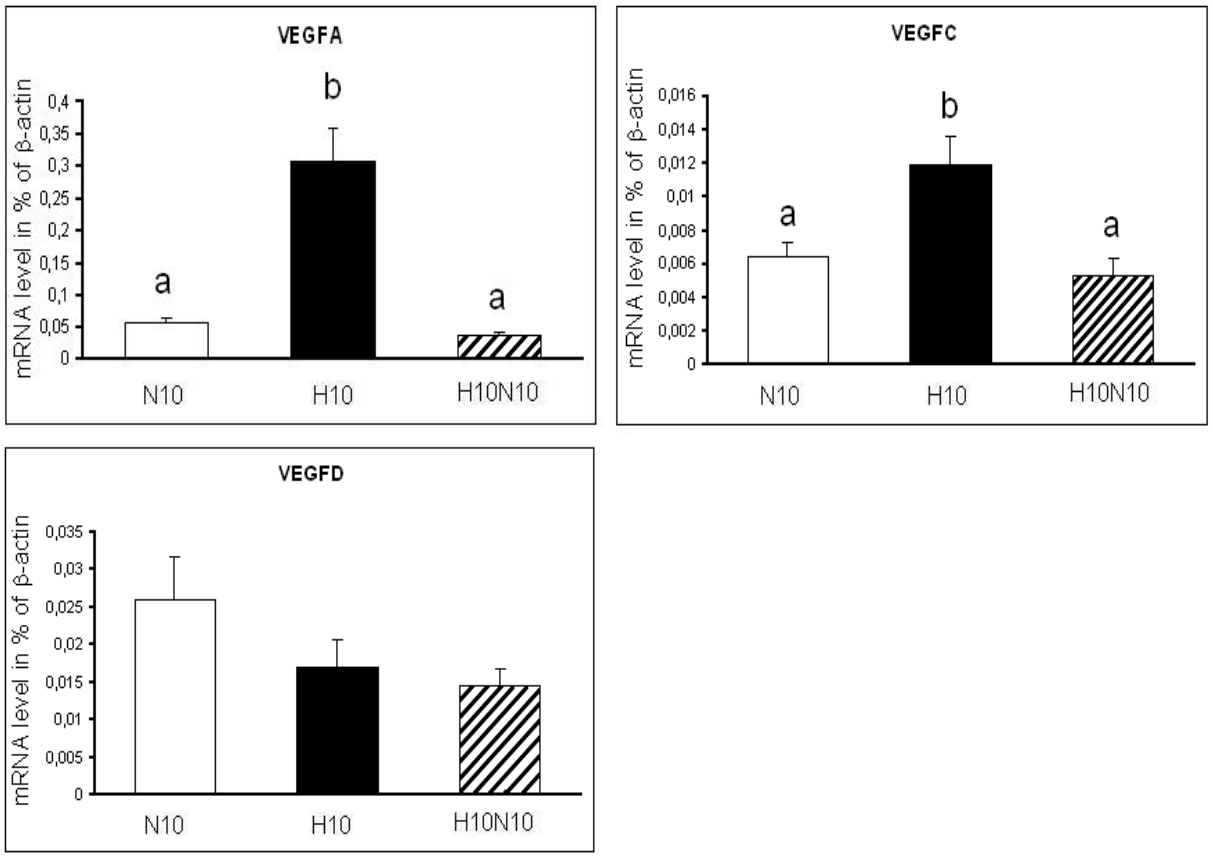

Figure 3.4. *Relative mRNA levels of VEGFA, VEGFC and VEGFD in the crucian carp brain, exposed to different oxygen regimes at 9℃. The data is normalized using β-actin as the internal reference gene. Different letters denote significant differences (Tukey post hoc test). For number of fish in each exposure group, see table 2.1. For statistical details, se appendix II.*

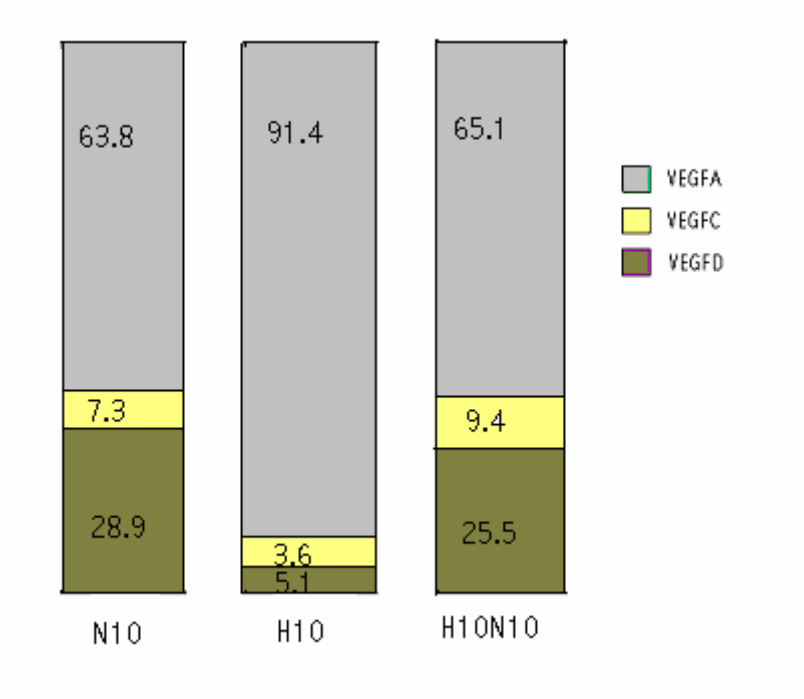

Figure 3.5. *Relative composition of VEGFA, VEGFC and VEGFD mRNA in normoxic, hypoxic and hypoxic normoxic crucian carp brain.*

3.5 Full length sequence of the VEGFA gene

Two different approaches were performed to obtain sequences from the VEGFA 3′ end. The first strategy was to perform RACE, which provided 20 sequences similar to the zebrafish $VEGFA_{121}$ variant, while it provided no sequences similar to $VEGFA_{165}$. Moreover, the obtained $VEGFA_{121}$ sequence displayed a curious property, its CDS (coding domain sequence) was not being defined by a stop codon. Since RACE failed to provide the $VEGFA_{165}$ sequence, ordinary PCR was used to obtain partial cloning of $VEGFA_{165}$ (appendix IV).

3.6 Immunohistochemistry and blood vessel quantification

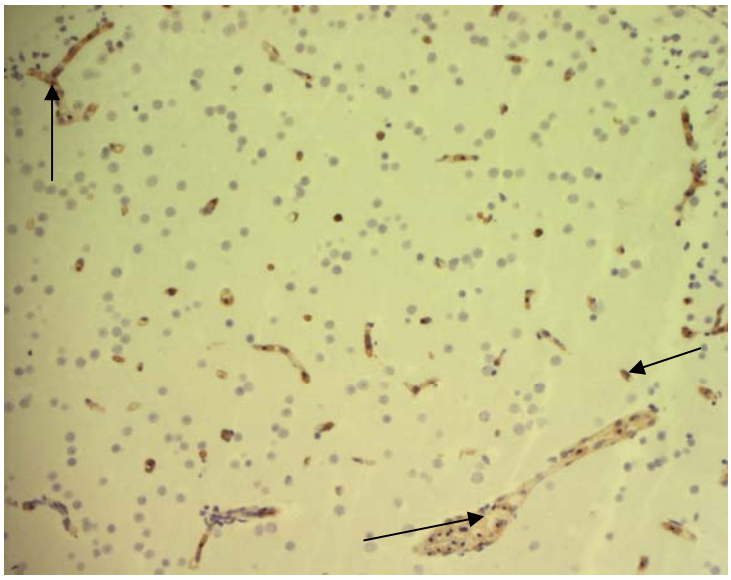

Figure 3.6. *Bloodvessels stained for Laminin*

From the second experiment, 20 fishes were used for immunohistochemical localisation of blood vessels. Of those fishes 8 had been exposed to 10 days of hypoxia, 6 to 10 days of hypoxia followed by 10 days of normoxia and the control group consisting of 6 animals that had been in normoxia for 10 days.

The experimental material was homogenous with respect to body size, so that fish weight did not differ between experimental groups or between males and females (two way ANOVA, effect of sex, P = 0.69; treatment effect, P = 0.54; sex/group interaction, P = 0.91). The frequency of males and females did not differ significantly between groups (chi-square test, P>0.05).

Blood vessels were easily identified by a brown residue due to the DAB polymerisation reaction (figure 3.6). All stained structures were included in the calculation of surface area per volume (S_v) and length per volume (L_v) described in section 2.13

The surface area per volume (S_v) was affected by both sex (P = 0.001) and experimental treatment (P < 0.001), and there was also significant interaction between the two variables (P = 0.009). Group means, S.E.M., and n are given in table 3.1. From this overview, it appears that males in general had lower S_v than females, with an overall mean (± S.E.M.) of 0.0119 ± 0.0004 (mm^2/mm^3) and 0.0131 ± 0.0009 (mm^2/mm^3), for males and females respectively (P < 0.001). Compared to controls in normoxia (overall mean ± S.E.M. = 0.015 ± 0.001), S_v was reduced in fish exposed to hypoxia (overall mean ± S.E.M. = 0.0112 ± 0.0004,

$P < 0.001$) as well as fish subjected to hypoxia followed by recovery in normoxia (overall mean ± S.E.M. = 0.0122 ± 0.0002, $P < 0.001$).

Table 3.1. *Blood vessel surface area per volume (S_v) of crucian carp telencephali after 10 days of normoxia, 10 days of hypoxia and 10 days of hypoxia followed by 10 days of reoxygenation in males, females and combined groups. Post-hoc tests for subgroups identified by both sex and treatment were not performed due to low numbers of individuals in the groups.*

	S_v mean (mm^2/mm^3)	S.E.M.	n
N10	**0,0148**	**0,0011**	**5**
males	0,0131	0,0005	3
females	0,0174	0,0008	2
H10	**0,0112**	**0,0004**	**9**
males	0,0102	0,0005	3
females	0,0118	0,0004	6
H10N10	**0,0122**	**0,0002**	**6**
males	0,0122	0,0003	4
females	0,0122	0,0001	2

The effect of exposure to hypoxia was also present for length per volume (L_v) ($P < 0.001$), while the effect of sex was absent for this variable ($P = 0.32$). Accordingly data for males and females were pooled and the resulting averages are graphed in figure 3.2. Even for this variable the normoxia group was significantly different from the other groups, while the trend towards recovery in the reoxygenation group (H10N10) did not reach statistical significance (post hoc significance levels given in figure 3.2).

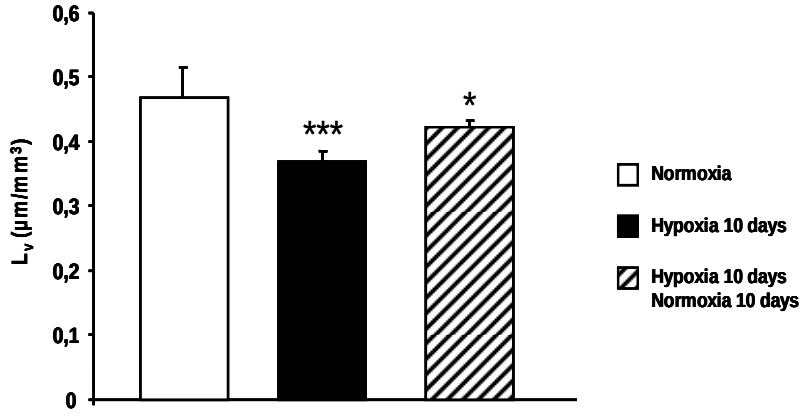

Figure 3.2. *Length of the blood vessel system per volume (L_v) in the telencephali of crucian carp kept in normoxia or hypoxia for 10 days or hypoxia for 10 days followed by normoxia for 10 days (Means + S.E.M.). Asterisks indicate a significant difference to controls kept in normoxia (* $P < 0.05$, *** $P < 0.001$)*

In figure 3.3 the regression between L_v and S_v is plotted with a common regression line for the three treatment groups. There were no between-group differences in regression line slopes (ANCOVA: N10 vs. H10: $t_{(10)} = 0.47$, P = 0.65; H10 vs. H10N10: $t_{(11)} = 0.65$, P = 0.51; N10 vs. H10N10: $t_{(7)} = 0.29$, P = 0.78). In pooled data this regression was highly significant ($R^2 = 0.50$, $p < 0.001$).

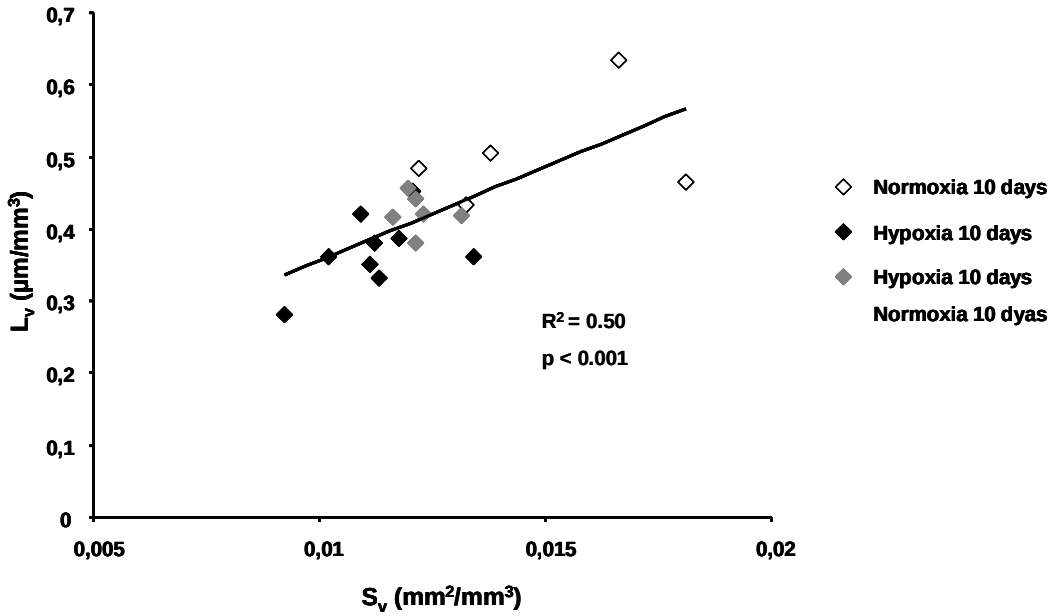

Figure 3.3. *The relationship between the blood vessel length per volume (L_v) and blood vessel surface area per volume (S_v). Data from all groups fall on the same regression line and are thus pooled.*

4 Discussion

In the present study the following genes were cloned from crucian carp; VEGFA, VEGFC, VEGFD (figure 3.1), HIF-1α, HIF-2α and FIH-1. Hypoxia exposure resulted in significant increases in the mRNA levels of VEGFA and VEGFC, while no changes were observed in VEGFD mRNA. The expression of FIH increased significantly. No changes were observed in HIF-1α and HIF-2α expression, but a trend towards a reduction in hypoxia was seen in HIF-1α mRNA.

With regard to vascular density in the telencephalon it was found that both surface area and total length of the blood vessel system were reduced in fish exposed to hypoxia.

4.1 Effect of hypoxia on mRNA levels in HIF, FIH and VEGF

While VEGF gene structure and regulation are less well characterized in fish compared to mammals, there are indications that these genes are also important for angiogenesis in fish. Thus VEGFA (Gong et al., 2004; Li et al., 2007), VEGFC (Roberts et al., 2004) and VEGFD (Song et al., 2007) have been cloned and characterized in zebrafish, where they appear to play important roles in vasculogenesis and angiogenesis. Previous results show that the expression of VEGF in mammals increases in hypoxia, and remain increased for an extended period (Kuo et al., 1999; Xue, 1998), but for how long depends on the species, hypoxia-protocol etc.

VEGFA showed the highest level of expression among the VEGF genes. It increased 6-fold in hypoxia and it constituted 90 % of the quantified VEGF expression in hypoxia (figure 3.5). The cDNA sequences of VEGFs obtained by cloning differed from VEGF in mammals, and even from other fish like zebrafish (figure 3.1). However, the deduced amino acid compositions of the VEGFs in crucian carp showed a high degree of similarity to those of zebrafish, suggesting that the functionalities of the VEGF genes are preserved.

That VEGF cDNA sequences differ between species also apply to their splice isoforms. While at least six splice isoforms of VEGFA exist in mammals (Roy et al., 2006b), in zebrafish four splice isoforms have been identified so far. These are named $VEGFA_{121}$, $VEGFA_{165}$, $VEGFA_{12345z\,678}$ and $VEGFA_{1234577a8}$. A variant similar to zebrafish $VEGFA_{121}$ was obtained in the crucian carp, and $VEGFA_{165}$ was partially cloned in the crucian carp (appendix IV). Two different strategies were tested to get to these sequences. RACE was

performed to obtain the 3′ end of VEGFA where the splice cassette is. This resulted in short sequences, which were similar to zebrafish $VEGFA_{121}$. However, these crucian carp $VEGFA_{121}$ sequences appeared odd, because no stop codon was found. The second approach was to create a sequence based on the cloned crucian carp VEGFA sequence and the 3′ end of the $VEGFA_{165}$ sequence from zebrafish (section 2.7.2), allowing partial cloning of $VEGFA_{165}$ in crucian carp. Gong et al. (2004) found in zebrafish that all tissues analyzed expressed high levels of $VEGFA_{121}$ and $VEGFA_{165.}$ They identified two new variants, $VEGFA_{12345z\,678}$ and $VEGFA_{1234577a8}$, where $VEGFA_{12345z\,678}$ was detected in heart and muscle while $VEGFA_{1234577a8}$ was only detected in zebrafish heart. These findings indicate that the different splice isoforms are not expressed in all tissue. It could be that their expression is restricted to particular organs or cell types. Since it was difficult to clone the $VEGFA_{165}$ variant in crucian carp brain, $VEGFA_{165}$ may have very low expression levels in this organ. Gong et al. (2004) concluded in their study that the CDS of zebrafish VEGFA was highly conserved between teleosts and mammals, while no obvious conservation was seen in the 5′ flanking regions. This suggests possible differences in VEGF gene regulation between fish and mammals.

The trend towards a reduction in VEGFD expression observed in hypoxia indicates that it does not have the same function in crucian carp as VEGFA and VEGFC. In humans VEGFD is both angiogenic and lymphangiogenic, while in mice it is proposed to be lymphangiogenic but not angiogenic due to the lack of a receptor (Baldwin et al., 2005). It has been shown in mice that expression of VEGFD induced growth of lymphatic vessels whereas blood vessels were unaffected (Veikkola et al., 2001). In addition, the zebrafish VEGFD gene is about 80 amino acids shorter than human and mouse VEGFD, and the crucian carp VEGFD was found to be even shorter, pointing at the possibility that crucian carp VEGFD has different functions than VEGFD in mammals.

The expression level of HIF-1α showed a trend towards a reduction in hypoxia, though not significant. No significant changes were seen in HIF-2α either. Changes seen in mRNA levels of HIF-1α and HIF-2α should not be emphasized too much because hypoxia induced changes in these factors primarily depend on increased protein levels (section 1.3). In crucian carp gills, the highest amount of HIF-1α protein is seen after 6 h of hypoxia, while after 48 h of hypoxia the level of HIF-1α protein is no longer elevated (Sollid et al., 2006). Chavez et al. (2000) examined the effects of hypoxia on HIF-1α and VEGF in the rat brain (Chavez et al., 2000). They found that during hypoxia the levels of HIF-1α protein remained significantly elevated for at least 14 days, and that they returned to normoxic levels within 21

days. The increased HIF-1α levels were paralleled by increased VEGFA transcript levels, indicating that HIF-1α targets VEGFA. In addition, the VEGFA gene has an HRE in its promoter region which HIF-α binds to and up-regulate VEGF expression (Hirota and Semenza, 2006; Storkebaum et al., 2004). While it is well established that VEGFA is a target gene for HIF-1α, it is possible that VEGFA expression can be induced by other genes than HIF-1α.

The expression levels of FIH increased 4-fold. FIH is known to reduce HIF-α transcriptional activity in normoxia, and Stolze et al. (2004) showed in mammalian cell lines that FIH contributes to control of HIF transcriptional response in hypoxia as well (Stolze et al., 2004). That both VEGFA and FIH increased in hypoxia in the present study might imply that the protein level of HIF-α also increases, due to negative feedback. Increased activity of FIH could start the process to reduce HIF-α activity. Obviously, protein levels of HIF-α have to be measured to verify that the expression of HIF-α increases in hypoxic crucian carp.

4.2 Vascularization

A decrease in both surface area and total length of the blood vessel system were seen in the present study. These findings are not in accordance with previous studies on the brain of mammals (e.g.(Dore-Duffy and La Manna, 2007; Drew et al., 2004; Harik et al., 1996; Harik et al., 1995; Mironov et al., 1994)), which show that hypoxia leads to angiogenesis with a near doubling of the capillary density (Dore-Duffy and La Manna, 2007). Xu and Severinghaus (1998) reported that the capillary density in rat brian increases significantly after one week of hypoxia, and a maximum increase reached after two weeks. Experiments in this field have mainly been performed on mice and rats, and to our knowledge no results are available from fish.

One could argue that the reduced vessel density can be explained by brain swelling. However, Van der Linden et al. (2001) demonstrated that the crucian carp brain does not swell during anoxia.

A possible explanation for the results in the present study is that there is no need to up-regulate the amount of vessels. Prolonged hypoxia results in a CBF increase in crucian carp, which could counteract the effect of reduced blood oxygen levels on oxygen delivery (Nilsson et al., 1994).

Moreover, it could be that making new blood vessels is too energy demanding for the crucian carp during hypoxia, and it is possible that VEGF has other functions beside blood vessel formation. It has been shown that VEGF has a direct neuroprotective effect in rats (Silverman et al., 1999), and studies performed on primary cultures of mice neurons increased neuronal viability (Jin et al., 2000).

The problem the crucian carp has to solve when it is exposed to hypoxia is to provide the tissue with enough oxygen. Vertebrates express HIF-α, and the function of this protein is to protect tissues from low oxygen levels. HIF-α is probably very important for local regulation of processes like angiogenesis, but a general increase in HIF-α levels, and all the pathways stimulated by it, could be undesirable for anoxia-tolerant animals exposed to general hypoxia. If angiogenesis (and erythropoiesis) is activated throughout the body, it could be that the hypoxic animal would end up as a "red ball" filled with blood and capillaries, wasting large quantities of energy building capillaries and erythrocytes and on pumping around an abnormally large blood volume. In view of this, it is tempting to suggest that there have to be mechanisms that inhibit HIF-α or HIF-α activated processes when the crucian carp becomes hypoxic. The increase in FIH seen in the present study indicates that FIH could be part of a system aimed at blocking HIF-α effects in hypoxic crucian carp. If VEGFA is involved in angiogenesis in crucian carp there have to be more factors than FIH involved in blocking angiogenesis, because VEGFA levels did increase and VEGFA is downstream of FIH inhibition.

4.4 Conclusions

Relative mRNA levels of VEGFA and VEGFC increased significantly in the crucian carp brain, while no changes were seen in VEGFD. VEGFA increased 6-fold and constitutes the largest part of the quantified VEGF expression. The VEGFA, VEGFC and VEGFD sequences obtained by cloning were different from VEGF in mammals, but similar to those of zebrafish. The crucian carp VEGFA splice isoforms were also similar to zebrafish $VEGFA_{121}$ and $VEGFA_{165}$.

The expression level of FIH increased 4-fold, while no significant changes in mRNA levels were seen in either HIF-1α or HIF-2α.

A significant hypoxia-induced decrease in vessel density was seen. The increase in VEGFA expression along with a reduction in blood vessel density can indicate that the crucian carp does not need additional vessels in hypoxia. On the contrary, it is possible that HIF-α effects have to be actively counteracted. Thus while HIF-1α is likely to be important in regulating regional oxygen supply by activating processes like angiogenesis, it could have undesirable effects during global hypoxia. If HIF-1α is allowed to activate angiogenesis in all tissues during hypoxia, the hypoxic animal could end up with having to pay too high costs for cell proliferation and for pumping a greatly increased blood volume. Thus, a well adapted facultative anaerob like the crucian carp may activate mechanisms aimed at turning off HIF-1α mediated processes during hypoxia.

References

Alberts B., Johnson A., Lewis J., Raff M., Roberts K., P. W. 2002. Molecular biology of the cell.1282-1283.

Bahary N, Goishi K, Stuckenholz C, Weber G, Leblanc J, Schafer CA, Berman SS, Klagsbrun M, Zon LI. 2007. Duplicate VegfA genes and orthologues of the KDR receptor tyrosine kinase family mediate vascular development in the zebrafish. Blood.

Baldwin ME, Halford MM, Roufail S, Williams RA, Hibbs ML, Grail D, Kubo H, Stacker SA, Achen MG. 2005. Vascular endothelial growth factor D is dispensable for development of the lymphatic system. Mol Cell Biol 25(6):2441-2449.

Bracken CP, Whitelaw ML, Peet DJ. 2003. The hypoxia-inducible factors: key transcriptional regulators of hypoxic responses. Cell Mol Life Sci 60(7):1376-1393.

Byrne AM, Bouchier-Hayes DJ, Harmey JH. 2005. Angiogenic and cell survival functions of Vascular Endothelial Growth Factor (VEGF). Journal of Cellular and Molecular Medicine 9(4):777-794.

Cai Z, Manalo DJ, Wei G, Rodriguez ER, Fox-Talbot K, Lu H, Zweier JL, Semenza GL. 2003. Hearts from rodents exposed to intermittent hypoxia or erythropoietin are protected against ischemia-reperfusion injury. Circulation 108(1):79-85.

Carmeliet P. 2003. Angiogenesis in health and disease. Nature medicine 9(6):653-660.

Chavez JC, Agani F, Pichiule P, LaManna JC. 2000. Expression of hypoxia-inducible factor-1alpha in the brain of rats during chronic hypoxia. J Appl Physiol 89(5):1937-1942.

Colognato H, Yurchenco PD. 2000. Form and function: the laminin family of heterotrimers. Dev Dyn 218(2):213-234.

Dayan F, Roux D, Brahimi-Horn MC, Pouyssegur J, Mazure NM. 2006. The oxygen sensor factor-inhibiting hypoxia-inducible factor-1 controls expression of distinct genes through the bifunctional transcriptional character of hypoxia-inducible factor-1alpha. Cancer Res 66(7):3688-3698.

Dore-Duffy P, La Manna JC. 2007. Physiologic angiodynamics in the brain. Antioxid Redox Signal 9(9):1363-1372.

Drew KL, Harris MB, LaManna JC, Smith MA, Zhu XW, Ma YL. 2004. Hypoxia tolerance in mammalian heterotherms. J Exp Biol 207(Pt 18):3155-3162.

Echteler SM. 1984. Connections of the Auditory Midbrain in a Teleost Fish, *Cyprinus carpio*.

Ellefsen S, Stensløkken K-O, Sandvik GK, Kristensen TA, Nilsson GE. *In prep.* Improved normalization of real time RT PCR data using an external RNA control.

Elvert G, Lanz S, Kappel A, Flamme I. 1999. mRNA cloning and expression studies of the quail homologue of HIF-2alpha. Mechanisms of development 87(1-2):193-197.

Ferrara N, Gerber HP, LeCouter J. 2003. The biology of VEGF and its receptors. Nature Medicine 9(6):669-676.

Gong B, Liang D, Chew TG, Ge R. 2004. Characterization of the zebrafish vascular endothelial growth factor A gene: comparison with vegf-A genes in mammals and Fugu. Biochimica et biophysica acta 1676(1):33-40.

Gordan JD, Bertout JA, Hu CJ, Diehl JA, Simon MC. 2007. HIF-2alpha promotes hypoxic cell proliferation by enhancing c-myc transcriptional activity. Cancer Cell 11(4):335-347.

Haddad JJ. 2002. Oxygen-sensing mechanisms and the regulation of redox-responsive transcription factors in development and pathophysiology. Respir Res 3:26.

Hallmann R, Horn N, Selg M, Wendler O, Pausch F, Sorokin LM. 2005. Expression and function of laminins in the embryonic and mature vasculature. Physiol Rev 85(3):979-1000.

Harik N, Harik SI, Kuo NT, Sakai K, Przybylski RJ, LaManna JC. 1996. Time-course and reversibility of the hypoxia-induced alterations in cerebral vascularity and cerebral capillary glucose transporter density. Brain research 737(1-2):335-338.

Harik SI, Hritz MA, LaManna JC. 1995. Hypoxia-induced brain angiogenesis in the adult rat. The Journal of physiology 485 (Pt 2):525-530.

Hirota K, Semenza GL. 2006. Regulation of angiogenesis by hypoxia-inducible factor 1. Crit Rev Oncol Hematol 59(1):15-26.

Ho QT, Kuo CJ. 2007. Vascular endothelial growth factor: Biology and therapeutic applications. Int J Biochem Cell Biol 39(7-8):1349-1357.

Hochachka PW, Lutz PL. 2001. Mechanism, origin, and evolution of anoxia tolerance in animals. Comp Biochem Physiol B Biochem Mol Biol 130(4):435-459.

Hu CJ, Wang LY, Chodosh LA, Keith B, Simon MC. 2003. Differential roles of hypoxia-inducible factor 1alpha (HIF-1alpha) and HIF-2alpha in hypoxic gene regulation. Mol Cell Biol 23(24):9361-9374.

Hylland P, Nilsson GE, Lutz PL. 1994. Time course of anoxia-induced increase in cerebral blood flow rate in turtles: evidence for a role of adenosine. J Cereb Blood Flow Metab 14(5):877-881.

Jin KL, Mao XO, Greenberg DA. 2000. Vascular endothelial growth factor: direct neuroprotective effect in in vitro ischemia. Proceedings of the National Academy of Sciences of the United States of America 97(18):10242-10247.

Johnston IA, Bernard LM. 1983. Utilization of the ethanol pathway in carp following exposure to anoxia. J Exp Biol 104:73-78.

Karkkainen MJ, Haiko P, Sainio K, Partanen J, Taipale J, Petrova TV, Jeltsch M, Jackson DG, Talikka M, Rauvala H, Betsholtz C, Alitalo K. 2004. Vascular endothelial growth factor C is required for sprouting of the first lymphatic vessels from embryonic veins. Nat Immunol 5(1):74-80.

Korsisaari N, Kasman IM, Forrest WF, Pal N, Bai W, Fuh G, Peale FV, Smits R, Ferrara N. 2007. Inhibition of VEGF-A prevents the angiogenic switch and results in increased survival of Apc+/min mice. Proceedings of the National Academy of Sciences of the United States of America.

Kuchler AM, Gjini E, Peterson-Maduro J, Cancilla B, Wolburg H, Schulte-Merker S. 2006. Development of the zebrafish lymphatic system requires VEGFC signaling. Curr Biol 16(12):1244-1248.

Kuo NT, Benhayon D, Przybylski RJ, Martin RJ, LaManna JC. 1999. Prolonged hypoxia increases vascular endothelial growth factor mRNA and protein in adult mouse brain. J Appl Physiol 86(1):260-264.

Lenfant C, Sullivan K. 1971. Adaptation to high altitude. The New England journal of medicine 284(23):1298-1309.

Li X-M, Yang J-M, Hu D-H, Hou F-Q, Zhao M, Zhu X-H, Wang Y, Li J-G, Hu P, Chen L, Qin L-N, Gao T-M. 2007. Contribution of Downregulation of L-type Calcium Currents to Delayed Neuronal Death in Rat Hippocampus after Global Cerebral Ischemia and Reperfusion. J Neurosci 27(19):5249-5259.

Lutz PL, Nilsson GE. 1997. Contrasting strategies for anoxic brain survival--glycolysis up or down. The Journal of experimental biology 200(Pt 2):411-419.

Lutz PL, Nilsson GE. 2004. Vertebrate brains at the pilot light. Respir Physiol Neurobiol 141(3):285-296.

Maharaj AS, D'Amore PA. 2007. Roles for VEGF in the adult. Microvasc Res.

Mironov V, Hritz MA, LaManna JC, Hudetz AG, Harik SI. 1994. Architectural alterations in rat cerebral microvessels after hypobaric hypoxia. Brain research 660(1):73-80.

Nilsson GE. 1990. Long-term anoxia in crucian carp: changes in the levels of amino acid and monoamine neurotransmitters in the brain, catecholamines in chromaffin tissue, and liver glycogen. The Journal of experimental biology 150:295-320.

Nilsson GE. 2001. Surviving anoxia with the brain turned on. News Physiol Sci 16:217-221.

Nilsson GE, Hylland P, Lofman CO. 1994. Anoxia and adenosine induce increased cerebral blood flow rate in crucian carp. The American journal of physiology 267(2 Pt 2):R590-595.

Nilsson GE, Lutz PL. 2004. Anoxia tolerant brains. J Cereb Blood Flow Metab 24(5):475-486.

Nilsson GE, Renshaw GM. 2004. Hypoxic survival strategies in two fishes: extreme anoxia tolerance in the North European crucian carp and natural hypoxic preconditioning in a coral-reef shark. The Journal of experimental biology 207(Pt 18):3131-3139.

Nolan T, Hands RE, Bustin SA. 2006. Quantification of mRNA using real-time RT-PCR. Nat Protoc 1(3):1559-1582.

Otrock ZK, Mahfouz RA, Makarem JA, Shamseddine AI. 2007a. Understanding the biology of angiogenesis: Review of the most important molecular mechanisms. Blood cells, molecules & diseases.

Otrock ZK, Makarem JA, Shamseddine AI. 2007b. Vascular endothelial growth factor family of ligands and receptors: review. Blood Cells Mol Dis 38(3):258-268.

Ramakers C, Ruijter JM, Deprez RH, Moorman AF. 2003. Assumption-free analysis of quantitative real-time polymerase chain reaction (PCR) data. Neurosci Lett 339(1):62-66.

Ratcliffe PJ. 2007. HIF-1 and HIF-2: working alone or together in hypoxia? J Clin Invest 117(4):862-865.

Roberts SB, McCauley LAR, Devlin RH, Goetz FW. 2004. Transgenic salmon overexpressing growth hormone exhibit decreased myostatin transcript and protein expression. Journal of Experimental Biology 207(21):3741-3748.

Roy H, Bhardwaj S, Babu M, Kokina I, Uotila S, Ahtialansaari T, Laitinen T, Hakumaki J, Laakso M, Herzig KH, Yla-Herttuala S. 2006a. VEGF-A, VEGF-D, VEGF receptor-1, VEGF receptor-2, NF-kappaB, and RAGE in atherosclerotic lesions of diabetic Watanabe heritable hyperlipidemic rabbits. Faseb J 20(12):2159-2161.

Roy H, Bhardwaj S, Yla-Herttuala S. 2006b. Biology of vascular endothelial growth factors. FEBS Lett 580(12):2879-2887.

Schena M, Heller RA, Theriault TP, Konrad K, Lachenmeier E, Davis RW. 1998. Microarrays: biotechnology's discovery platform for functional genomics. Trends Biotechnol 16(7):301-306.

Senger DR, Connolly DT, Van de Water L, Feder J, Dvorak HF. 1990. Purification and NH2-terminal amino acid sequence of guinea pig tumor-secreted vascular permeability factor. Cancer Res 50(6):1774-1778.

Senger DR, Perruzzi CA, Feder J, Dvorak HF. 1986. A highly conserved vascular permeability factor secreted by a variety of human and rodent tumor cell lines. Cancer Res 46(11):5629-5632.

Shi L, Reid LH, Jones WD, Shippy R, Warrington JA, Baker SC, Collins PJ, de Longueville F, Kawasaki ES, Lee KY, Luo Y, Sun YA, Willey JC, Setterquist RA, Fischer GM,

Tong W, Dragan YP, Dix DJ, Frueh FW, Goodsaid FM, Herman D, Jensen RV, Johnson CD, Lobenhofer EK, Puri RK, Schrf U, Thierry-Mieg J, Wang C, Wilson M, Wolber PK, Zhang L, Amur S, Bao W, Barbacioru CC, Lucas AB, Bertholet V, Boysen C, Bromley B, Brown D, Brunner A, Canales R, Cao XM, Cebula TA, Chen JJ, Cheng J, Chu TM, Chudin E, Corson J, Corton JC, Croner LJ, Davies C, Davison TS, Delenstarr G, Deng X, Dorris D, Eklund AC, Fan XH, Fang H, Fulmer-Smentek S, Fuscoe JC, Gallagher K, Ge W, Guo L, Guo X, Hager J, Haje PK, Han J, Han T, Harbottle HC, Harris SC, Hatchwell E, Hauser CA, Hester S, Hong H, Hurban P, Jackson SA, Ji H, Knight CR, Kuo WP, LeClerc JE, Levy S, Li QZ, Liu C, Liu Y, Lombardi MJ, Ma Y, Magnuson SR, Maqsodi B, McDaniel T, Mei N, Myklebost O, Ning B, Novoradovskaya N, Orr MS, Osborn TW, Papallo A, Patterson TA, Perkins RG, Peters EH, Peterson R, Philips KL, Pine PS, Pusztai L, Qian F, Ren H, Rosen M, Rosenzweig BA, Samaha RR, Schena M, Schroth GP, Shchegrova S, Smith DD, Staedtler F, Su Z, Sun H, Szallasi Z, Tezak Z, Thierry-Mieg D, Thompson KL, Tikhonova I, Turpaz Y, Vallanat B, Van C, Walker SJ, Wang SJ, Wang Y, Wolfinger R, Wong A, Wu J, Xiao C, Xie Q, Xu J, Yang W, Zhang L, Zhong S, Zong Y, Slikker W, Jr. 2006. The MicroArray Quality Control (MAQC) project shows inter- and intraplatform reproducibility of gene expression measurements. Nat Biotechnol 24(9):1151-1161.

Shoubridge EA, Hochachka PW. 1980. Ethanol: novel end product of vertebrate anaerobic metabolism. Science 209(4453):308-309.

Silverman WF, Krum JM, Mani N, Rosenstein JM. 1999. Vascular, glial and neuronal effects of vascular endothelial growth factor in mesencephalic explant cultures. Neuroscience 90(4):1529-1541.

Sollid J, De Angelis P, Gundersen K, Nilsson G. 2003. Hypoxia induces adaptive and reversible gross morphological changes in crucian carp gills. J Exp Biol 206(20):3667-3673.

Sollid J, Kjernsli A, De Angelis PM, Rohr AK, Nilsson GE. 2005. Cell proliferation and gill morphology in anoxic crucian carp. Am J Physiol Regul Integr Comp Physiol 289(4):R1196-1201.

Sollid J, Rissanen E, Tranberg HK, Thorstensen T, Vuori KAM, Nikinmaa M, Nilsson GE. 2006. HIF-1 alpha and iNOS levels in crucian carp gills during hypoxia-induced transformation. Journal of Comparative Physiology B-Biochemical Systemic and Environmental Physiology 176(4):359-369.

Song M, Yang H, Yao S, Ma F, Li Z, Deng Y, Deng H, Zhou Q, Lin S, Wei Y. 2007. A critical role of vascular endothelial growth factor D in zebrafish embryonic vasculogenesis and angiogenesis. Biochemical and biophysical research communications 357(4):924-930.

Spike RC, Kerr R, Maxwell DJ, Todd AJ. 1998. GluR1 and GluR2/3 subunits of the AMPA-type glutamate receptor are associated with particular types of neurone in laminae I-III of the spinal dorsal horn of the rat. European Journal of Neuroscience 10(1):324-333.

Stolze IP, Tian YM, Appelhoff RJ, Turley H, Wykoff CC, Gleadle JM, Ratcliffe PJ. 2004. Genetic analysis of the role of the asparaginyl hydroxylase factor inhibiting hypoxia-inducible factor (HIF) in regulating HIF transcriptional target genes. The Journal of biological chemistry 279(41):42719-42725.

Storkebaum E, Lambrechts D, Carmeliet P. 2004. VEGF: once regarded as a specific angiogenic factor, now implicated in neuroprotection. Bioessays 26(9):943-954.

Veikkola T, Jussila L, Makinen T, Karpanen T, Jeltsch M, Petrova TV, Kubo H, Thurston G, McDonald DM, Achen MG, Stacker SA, Alitalo K. 2001. Signalling via vascular endothelial growth factor receptor-3 is sufficient for lymphangiogenesis in transgenic mice. The EMBO journal 20(6):1223-1231.

Wang GL, Jiang BH, Rue EA, Semenza GL. 1995. Hypoxia-inducible factor 1 is a basic-helix-loop-helix-PAS heterodimer regulated by cellular O2 tension. Proceedings of the National Academy of Sciences of the United States of America 92(12):5510-5514.

Wigle JT, Oliver G. 1999. Prox1 function is required for the development of the murine lymphatic system. Cell 98(6):769-778.

Woolard J, Wang WY, Bevan HS, Qiu Y, Morbidelli L, Pritchard-Jones RO, Cui TG, Sugiono M, Waine E, Perrin R, Foster R, Digby-Bell J, Shields JD, Whittles CE, Mushens RE, Gillatt DA, Ziche M, Harper SJ, Bates DO. 2004. VEGF165b, an inhibitory vascular endothelial growth factor splice variant: mechanism of action, in vivo effect on angiogenesis and endogenous protein expression. Cancer Res 64(21):7822-7835.

Xu K, Puchowicz MA, LaManna JC. 2004. Renormalization of regional brain blood flow during prolonged mild hypoxic exposure in rats. Brain research 1027(1-2):188-191.

Xue H. 1998. Identification of major phylogenetic branches of inhibitory ligand-gated channel receptors. J Mol Evol 47(3):323-333.

Yaniv K, Isogai S, Castranova D, Dye L, Hitomi J, Weinstein BM. 2006. Live imaging of lymphatic development in the zebrafish. Nature medicine 12(6):711-716.

Appendices:

Appendix I **Reagents, equipement and software**

Appendix II **Statistical details**

Appendix III **Sequences and real-time RT-PCR products**

Appendix IV **$VEGFA_{121}$ and $VEGFA_{165}$**

Appendix V **Immunohistochemical staining technique**

Appendix I

Reagents, equipement and software

The following reagents, equipement and software were used in this thesis.

Reagents (product, catalogue number and manufacturer)

Advtantage 2 polymerase mix, Clontech Laboratories Inc., Mountain View, USA

Agarose, SeaKem®, 50004, Cambrex

Ampicillin (D[-]-α-Aminobenzylpenicillin), A-9518, Sigma

Antibody Diluent, S0809, DakoCytomation

Anti-Laminin 1.20, L9393, Sigma

Anti-Laminin 1:400, Z0097, DakoCytomation

Chloroform, C2432, Sigma

DAB+, K3468, DakoCytomation

DEPC (dietyl pyrokarbonat), SD5758, Sigma

EnVision+ System, K4011, DakoCytomation

Etidium bromide, 443922U, BHD-Electron

Eukitt, O. Kindler GmbH & co., Germany

FastStart Taq Polymerase, 03515885001, Roche Diagnostics

Generacer^{TM} Kit, version L, Invitrogen

Haematoxylin, S3301, DakoCytomation

Hydrogen peroxide 0.03%, S2001, DakoCytomation

LightCycler®FastStart DNA Master^{PLUS} SYBR Green I, 03515885001, Roche Diagnostics

Menzel gläser SuperFrost (R) Plus, Menzel GmbH & Co KG, Saarbrückener Str. 248, Germany

pGEM®-T Easy Vector Systems, A1360, Promega

Proteinase K 40x, S2019, DakoCytomation

RNA 6000 Nano Lab Chip® Kit, 5065-4474, Agilent

RNA 6000 Nano Reagents PartI, 5067-1511, Agilent

SOC medium, 15544-034, Invitrogen

Superscript^{TM} III Reverse Transcriptase, 18080-(044), Invitrogen

T7 RNA Polymerase, 18033-019, Invitrogen

TRIzol® Reagent, 15596-018, Invitrogen

TURBO DNA-free™ Kit, Cat #1907, Ambion

X-Gal, V3941, Promega

Equipment (product, catalogue number/model and manufacturer)

Agilent Bioanalyzer, G2938B, Agilent

BioDoc-It™ System, UVP

Eppendorf centrifuge, 5417R, Eppendorf

Finnpipettes, U23386, T27033, T27388, T28301, Thermo Labsystems

Homogenizer, Duall® 22, Kontes glass

Homogenizer, Ultra-Turrax T8, IKA

LightCycler Capillaries (20 µl), 11909339001, Roche Diagnostics

LightCycler Carousel Centrifuge, 12189682001, Roche Diagnostics

LightCycler 2.0 Instrument, 03531414201, Roche Diagnostics

NanoDrop®, Model ND-1000, NanoDrop Technologies

N_2-gas, AGA

Software

AxioVision, Release 4.5, Des 2005

Bioanalyzer 2100 expert, version B.01.02 SII36, Agilent Technologies

GraphPad InStat 3.06, GraphPad Software Inc.

ImageJ 1.37v, (http://rsb.info.nih.gov/ij/), Wayne Rasband, National Institutes of health, USA

LightCycler3 Data Analysis, version 3.5.28, Idaho Technology Inc.

LightCycler3 Front, version 3.5.17, Idaho Technology Inc.

LightCycler3 Probe Software, version 1.0, Idaho Technology Inc.

LightCycler3 Run, version 5.32, Idaho Technology Inc/ Roche Diagnostics

NanoDrop 3.0.1, Coleman Technologies Inc.

Freeware

BioEdit Sequence alignment editor, version (http://www.mbio.ncsu.edu/BioEdit/page2.html), © 1997-2005 by Tom Hall

Clustal X, version 1.83, Feb 2003 (ftp://ftp-igbmc.u-strasbg.fr/pub/ClustalX/)

GeneDoc, version 2.6.002 (http://www.psc.edu/biomed/genedoc/) © 2000 by Karl Nicholas

GENSCAN (http://genes.mit.edu/GENSCAN.html) © 1997-2005 by Christopher Burge

LinReg, version 7.5, Feb 2004 (Available on request; e-mail; bioinfo@amc.uva.nl; subject: LinReg PCR), Dr. J. M. Ruijter, Department og Anatomy and Embryology, Academic Medical Centre, Amsterdam, Netherlands

Primer3 (http://frodo.wi.mit.edu/cgi-bin/primer3/primer3_www.cgi), © 2004 Whitehead Institute for Biomedical Research

TreeView (Win 32) (http://taxonomy.zoology.gla.ac.uk/rod/rod.html) © Roderic D. M. Page, 2001

Appendix II

Statistical details

Statistical details of each gene of interest. The reference explains where in this thesis a graphical presentation is found.

Gene of interest	Test	P-value	Post-test	n in each group (N10,H10,H10N10)	Reference
HIF-1α	Two way ANOVA	0.06		6, 5, 6	Figure 3.1
HIF-2α	Two way ANOVA	0.70		6, 5, 6	Figure 3.1
FIH-1	Two way ANOVA	0.002	Tukey post Hoc test	6, 5, 5	Figure 3.3
VEGFA	Two way ANOVA	< 0.01	Tukey post Hoc test	6, 5, 5	Figure 3.4
VEGFC	Two way ANOVA	0.005	Tukey post Hoc test	6, 5, 5	Figure3.4
VEGFD	Two way ANOVA	0.20		6, 5, 6	Figure 3.4

Appendix III

VEGF sequences

The following sequences of crucian carp (Cc) were obtained by cloning and sequencing of cDNA. The real-time RT-PCR products from each gene are highlighted in red.

Cc_VEGFA_303bp **real-time RT-PCR product: 145-301**

1 CTGTTAAGGCTGCCCACATACCTAAAGAAGGGATGAAGGGCAAAAA 46
47 TGAGGTGATTCCCTTCATGGATGTGTACAAAAAGAGTGCATGTAAGA 93
94 CGCGAGAGTTGCTGGTAGACATCATTCAGGAGTATCCTGACGAGATC 140
141 GAGCACACCTACATCCCGTCCTGTGTGGTTCTCATGCGCTGTGCAGG 187
188 CTGCTGCAACGACGAAGCACTCGAGTGTGTCCCTACAGAGACCCGCA 234
135 ACGTCACCATGGAGGTACTGCGAGTCAAACAACGTGTTTCGCAGCAT 281
282 AATTTTCAACTGAGTTTCACAG 303

Cc_VEGFC_682bp **real-time RT-PCR product: 43-297**

1 TATAAACCACCCTGCGTGTCTGTCTACAGATGTGGGGGCTGCTGTAA 47
48 CAGTGAGGAGCAAGTGTGCAAGAACATGAGCACTTCATACGTCAGTA 94
95 AGACGTTGTTTGAAATCACAGTTCCTATGAAGTATGGGCCCAAGCCA 141
142 GTCACCATAAGCTTCGCCAACCACACTTCCTGCAGCTGTTTGTCAAAA 189
190 CAGGATTTGTACCGACAGCAGCACTCAATAATTCGAAGGGCCTTACC 236
237 AGAATGTCATGTGGCAAATAAAACATGCCCAAAGAATCACAGCTGGA 283
284 GTAATCGCTTGTGTAGATGTGTGCCACTACCCGACACCCTCTTTTCACA 332
333 GCCAAATTATGCAGACTTTGAGCAGGACTTCTGCGGTCCCGACAAAGA 380
381 GCTGGATGAAGAGACTTGTCAGTGTGTATGCCGAAAACAGCTGCGAAC 428
429 GGCAGGCTGTGGACCGCACCACTATTTGGACAAGAACACCTGTCAGTG 476
477 TGTGTGTAAAGCGAAGCCTTCTTCCTGCAGGCCTCAACAGAGCTTCAA 524
525 CAAGGACACCTGCCATTGCACCTGCACCAAGGTGTGTCCTAGCAGTCA 572
573 GCCTCTCAACCGCACCAAATGTGTGTGTGAATGCACAGAGTCCCCTAA 620
621 CAAGTGCTTCTTAAAAGGAAGGCGGTTCCACCCGGGCACATGCAGTTG 668
669 TGTAAGGCCACCGT 682

Cc_VEGFD_705bp **real-time RT-PCR product: 377-636**

1 CTGTATGTCAGATTGATGCTGGCCGTGGACGCCTACAGACCCCAGAGA 48
49 GACATAAACCAGGAGAGGTGGGAACAGGAAATAAGGGAAGCTGGGAG 95
96 TCTGGATGAGCTTATGATGTTGACCGAATACCCGGACTGGAAGCTGKG 143
144 GAGATGCAGATTTAAGCTGAAGCACTTTGAATATGTCAATCCGCTTGAG 192
193 AACCGCAGGTCAACACGCTATGCTGCCACATCATTCAGCCCAGAGATTC 241
242 TTAAAGATATTGATGACGAATGGCAGAAAACACAGTGTATGCCCAGAGA 290
291 GACATGTGTAGATGTGGCTAAAGAGCTGGGCACCAGTACGGCTGTGTTC 339
340 TTTAAGCCCCCGKGTGTCTCTGTCTTCAGGTGTGGCGGCTGCTGCAACAA 389
390 AGAGGGAGTTACCTGCCGTAATACAAGCGTGACTTATATTAATAAAACT 438
439 ATTTTGAGTGTGAGTCTGGCTCCGTATAAATCTGGACCAGAGCCCGTGCT 488
489 GGTGAAAATTGCCAATCACACTGAGTGCATGTGCCAGGAACATACGCTG 537
538 ATTCGCAGACATGTTCGTGAGAAGCACAAGAAGAGTTGCTCTCCTACAC 586
587 GTAAGCCAGAAGACAAGAGGCTATGCAACAGAGGTTTAATATGGGACT 634
635 GGATGGCGGAGCGATGTGTGACGTACCCCTCCAGTAAACAAGATCCTCC 683
684 GTCTACAGTCAGGGAAGAGGAC 705

Appendix IV

VEGFA$_{121}$ and VEGFA$_{165}$

An amino acid alignment showing the human (hs) VEGFA$_{121}$ and VEGFA$_{165}$ sequences and comparing them to analogous sequences from zebrafish (dr) and crucian carp (cc). Complete CDS are shown for hs and dr. In all sequences but the hs VEGFA$_{165}$ dots refer to conserved amino acid sequences, letters refer to differences in amino acids and hyphens refer to the lack of amino acids. The question marks refer to uncharacterized amino acids in the crucian carp sequences.

```
                    *        20         *        40         *
hsVEGFA165 : MNFLLSWVHWSLALLLYLHHAKWSQAAPMAEGGGQNHHEVVKFMDVYQRS :  50
hsVEGFA121 : ................................................. :  50
drVEGFA165 : ..L..YL.QLF..A..H.SAV.----.H.PKE..KSKND..P.....K.. :  47
drVEGFA121 : ..L..YL.QLF..A..H.SAV.----.H.PKE..KSKND..P.....K.. :  47
ccVEGFA165 : ???????????????A..H.SAV.----.H.PKE.MKGKN...P.....K.. :  34
ccVEGFA121 : ???????????????A..H.SAV.----.H.PKE.MKGKN...P.....K.. :  34

                   60         *        80         *       100
hsVEGFA165 : YCHPIETLVDIFQEYPDEIEYIFKPSCVPLMRCGGCCNDEGLECVPTEES : 100
hsVEGFA121 : ................................................. : 100
drVEGFA165 : A.KTR.L....I........HT.I....V....A......A.......TR :  97
drVEGFA121 : A.KTR.L....I........HT.I....V....A......A.......TR :  97
ccVEGFA165 : A.KTR.L....I........HT.I....V....A......A.......TR :  84
ccVEGFA121 : A.KTR.L....I........HT.I....V....A......A.......TR :  84

                    *       120         *       140         *
hsVEGFA165 : NITMQIMRIKPHQGQHIGEMSFLQHNKCECRPKKD-RARQENPCGPCSER : 149
hsVEGFA121 : ..........................................-.....--------- : 140
drVEGFA165 : ..........QRVS..NF....T..T.......AEV...K..H.E..... : 147
drVEGFA121 : ..........QRVS..NF....T..T.......AEV...K.--------- : 138
ccVEGFA165 : ..........QRVS..NF....T..T.......VEV.S.K..H.E..... : 134
ccVEGFA121 : ..........QRVS..NF....T..T.......VEV.S.K---------- : 124

                   160         *       180         *
hsVEGFA165 : RKHLFVQDPQTCKCSCKNTDSRCKARQLELNERTCRCDKPRR : 191
hsVEGFA121 : ------------------------------------..... : 147
drVEGFA165 : ..R......L.......F.QMQ..S............E...- : 188
drVEGFA121 : -----------------------------------..E...- : 144
ccVEGFA165 : ..R......L.......F.QMQ..S.R.......??????   : 168
ccVEGFA121 : ----------------------------------.KK.K.- : 130
```

Appendix v

Paraffin embedding

The procedure in the machine is as followed:

1. The tissue was first dehydrated; defined as replacment of water by hydrofobic liquids. This was done by using an increasing alcohol concentration, from 70% until absolute alcohol. The time should be as short as possible to avoid shrinkage (average time about five and a half hour; 70% alc 30 minutes, 96% alc 1 hour, Abs alc 4 times 1 hour).
2. The alcohol is then replaced by a clarifying agent, xylene, which is soluble both in alcohol and paraffin (two times 1 hour).
3. Xylene is replaced by liquid paraffin which has a melting point at about 60 degrees (4 times 45 minutes).

These three steps are done in the machine under pressure and high degree to decrease the penetrating time and to get a good infiltration of the paraffin.